Integrated Fieldwork 2020

WP1: Three-Dimensional Reference Frame via GNSS Observations

Supervisors:

Prof. Dr. James Foster

Dr. Karim Douch

Dipl. Ing. Ron Schlesinger

Students

Ziqing Yu

University of Stuttgart
Germany

Contents

1. Introduction

In order to get the UTM coordinates of the points near the hysolar building, the GNSS observations took place on 3 points near the building and 3 points with know coordinates. The data were edited and calculated with Leica Geooffice. The results of the observations are the UTM ETRS89 coordinates and the ellipsoidal height of the FP1, FP2, FP3 near the Building.

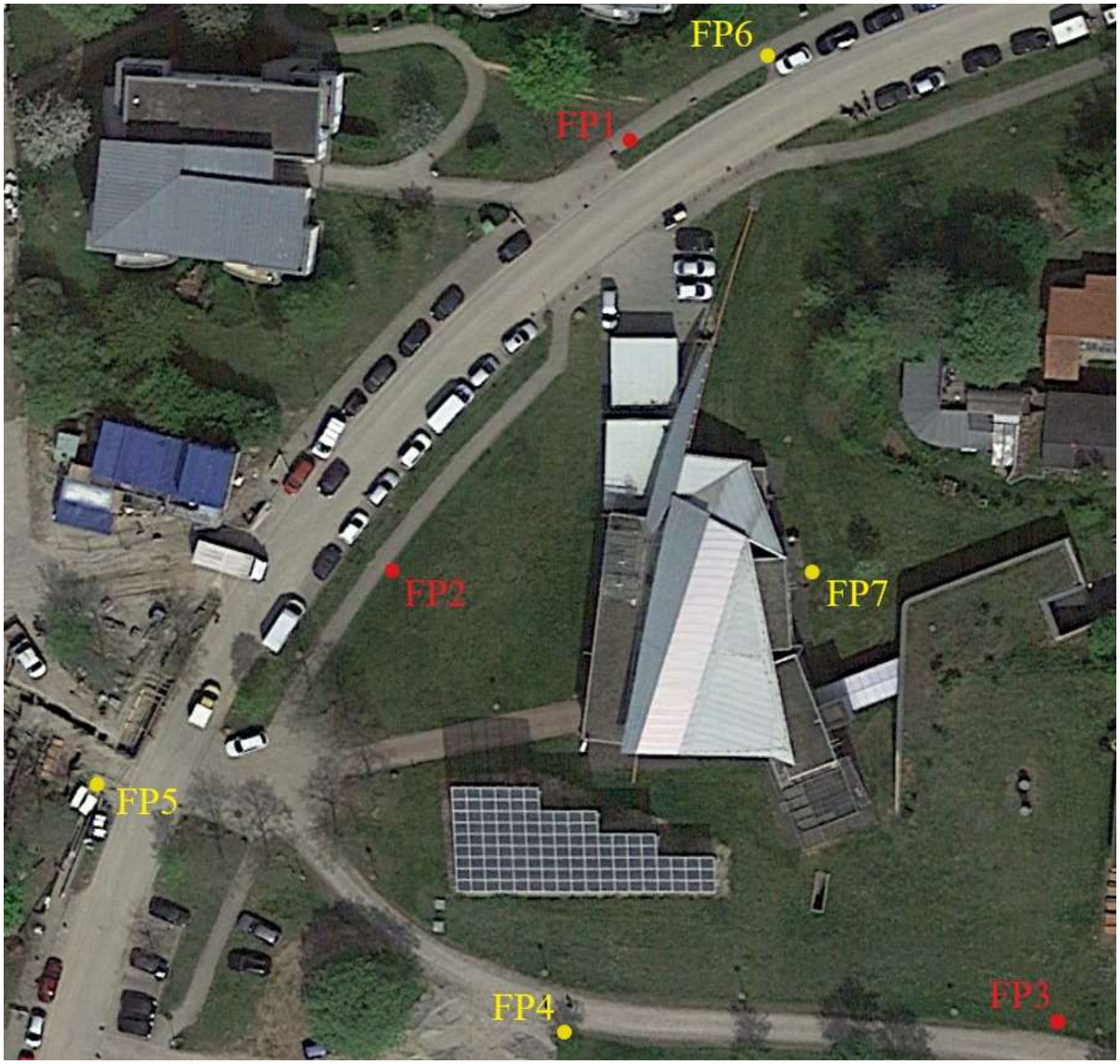

2. Process

There are 6 points in total, 3 of them near the building and the other with known coordinates. Each of these points should be observed at least 3 times. We have 4 measure groups, so the observation took place with 5 sessions in 2 days.

All the groups should measure at least 1 hour in same time. To make sure of that, all groups switched the on the observation and documented their start time direct after they reached the point in every session. Then all groups stopped after the last group had been observed 1 hour.

It was planned that all the groups communicated with Walkie-Talkie. However, the distance between the Hysolar building and PF4 was too far for the Walkie-Talkie to work. The alternative was the WhatsApp.

After that, all the data were collected and processed in Leica Geooffice, the data were adjusted, the baselines were created. The network was performed and the coordinates and the errors were calculated.

The UTM coordinates were delivered to WP2 and WP4, the ellipsoidal heights were given to WP3 and WP4.

3. Problems

During the observation, we met some problems and also made some mistakes.

1. There is a honeycomb in the Pillar of PF7, when we set up the GNSS receiver, we needed to be very careful.

2. The height type of receiver are wrongly documented. There are 2 kinds of type of the height: pillar and the tripods, some receivers were on the tripods but the heights were documented as “pillar”, which would cause 36 cm difference.

3. Some groups forgot to switch off the last observation and went to the next station directly. So, the data in this period need to be deleted manually.

4. Results

At the very beginning, all 6 points were adjusted, the coordinates calculated from Leica Geooffice:

Point	East	North	Ellipsoidal height (GRS80)
PF4	32506345.459	5398933.288	474.107
PF7	32506572.617	5398945.291	474.364
PF10	32507243.832	5399150.820	489.694
FP1	32507095.366	5398980.027	502.631
FP2	32507072.170	5398935.852	503.018
FP3	32507140.526	5398883.513	506.246

The errors:

Point	Std East	Std North	Std Height
PF4	0,006	0,006	0,005
PF7	0,003	0,002	0,003
PF10	0,005	0,002	0,004
FP1	0,003	0,003	0,003
FP2	0,002	0,003	0,002
FP3	0,003	0,004	0,004

The adjusted network:

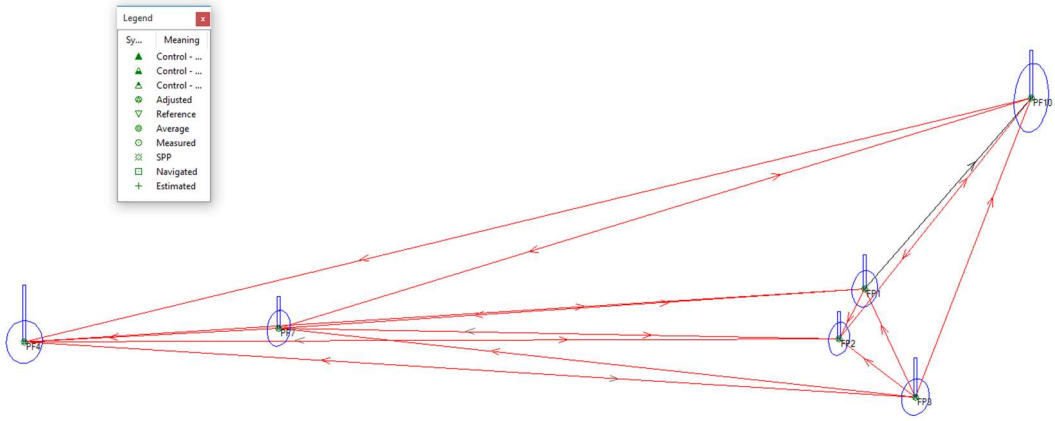

In principle we should set PF4, PF7 and PF10 as fix points and adjust other new points, but the old coordinates of PF4, PF7 and PF10 are measured long time ago and transformed from Gauß-Krüger coordinate system, when mistakes during the transformation can happen. We used the SAPOS data to verify the coordinates and found the newly calculated coordinates are better (5-centimeter difference). So, we decide to use the result above directly.

Integrated Fieldwork 2020

WP2: Creation of a 3D Network by Total Station

Supervisor: Gabriel Kerekes

Student: Junyang Gou, 3218006

University of Stuttgart
Germany

Contents

Chapter 1

Process

1.1 The field measurement

The field measurement is mainly divided into two parts: Team A, B and C were responsible for measuring on two station points each team, for establishing a local reference system (24. June – 29. June). Team D was responsible for measuring the coordinates of the checkpoints (06. July) required by WP5 based on the existing fix points.

Because the data processing of WP1 and WP3 takes time, the UTM coordinates and the DHHN heights of the network could not be provided before 06. July. But the field measurement of WP5 started on 06. July, and they need the coordinates of the checkpoints for their measurements. Therefore, Team D measured the local coordinates of the required checkpoints based on the local reference system. After that, when we have the global reference system, the global coordinates of checkpoints were later obtained through transformation.

1.2 The local network frame

After 29. June, all the information for the local network adjustment is gathered. The local network adjustment has been done by using *JAG3D*.

First, all data must be preprocessed into column-based data in order to be imported in *JAD3D*, as shown in Fig. 1.1. When all data are imported, we should manually enter the names of all the points in the window 'New points'. Then, a free network adjustment is conducted with a complete trace minimization. Later we should guarantee the network quality by checking the variance component estimations, as shown in Fig. 1.2. From this figure, we can find that the quality of the first adjustment is not sufficient. The factor $1/\sigma^2$ should between 0.8 and 1.3. The components, which do not fulfill this requirement, include some blunders.

When we go to the individual measurements, we can also find some statistic parameters, which could help us to determine the blunders. The highlights are with respect to the estimated gross error ∇, which is detected in the observations through mutual self-control (internal reliability). If the single measurement is red, it is considered as a blunder in the current network. It does not mean that those measurements are really errors, but just conflict with the current network configuration. If we enable some of them, the others could be acceptable because the conflict is already solved. We should enable some measurement whose

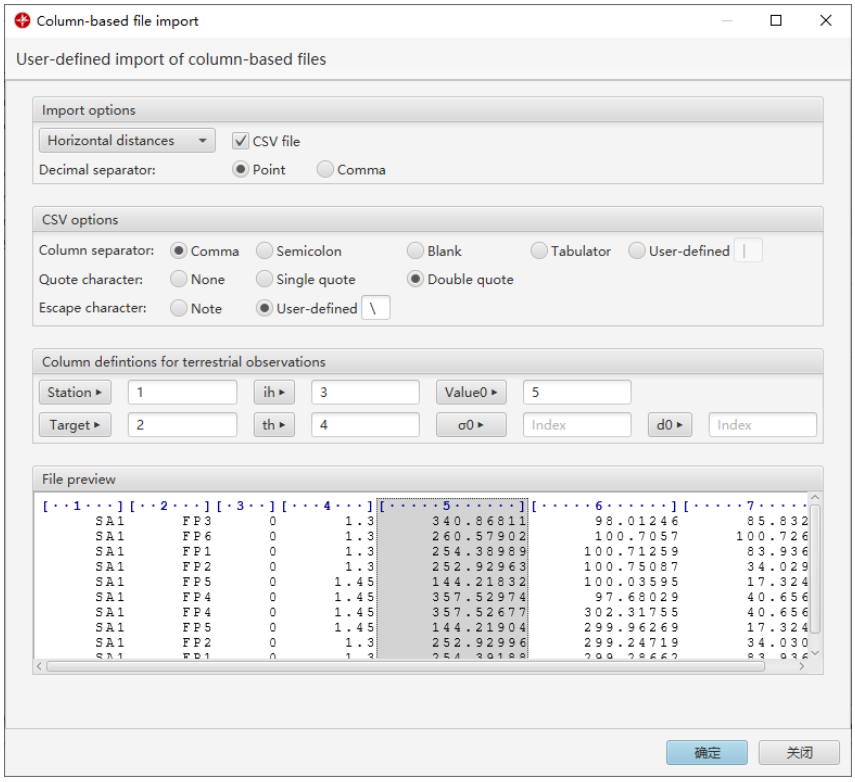

Figure 1.1: *The window of import data*

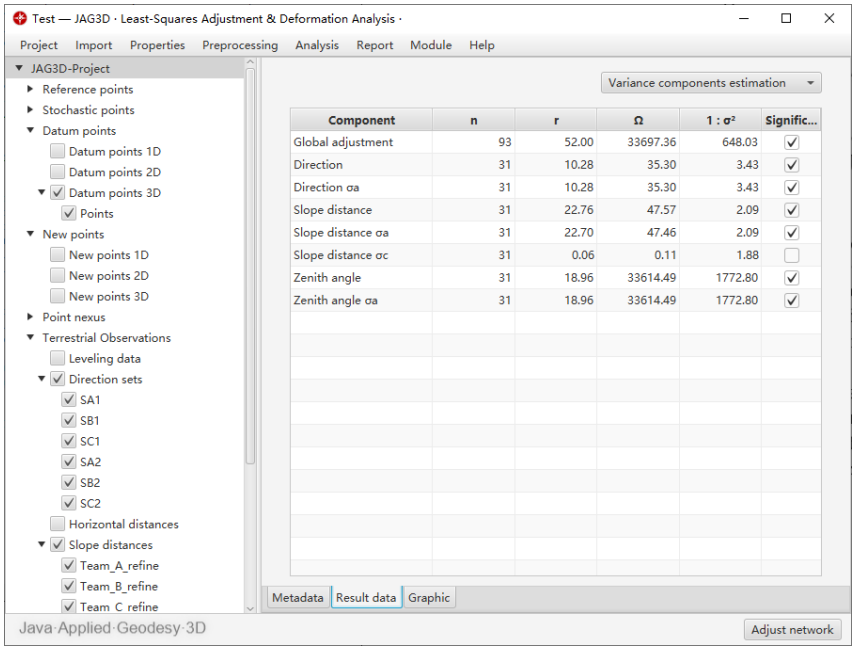

Figure 1.2: *The network adjustment results of the first adjustment*

∇ and r are high, where r is the redundancy. The network configuration will not be destroyed, when some measurements with high redundancy are enabled.

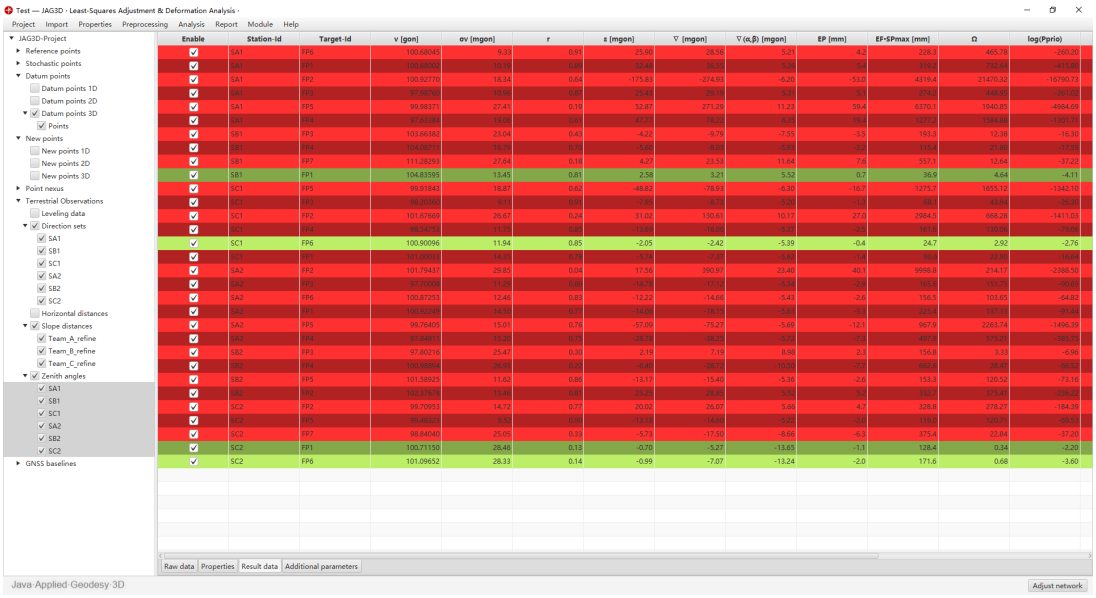

Figure 1.3: *The result data of zenith angles after the first adjustment*

This process is an iterative process, which means, we should not enable too many measurements at once. We should enable some measurements, which have the biggest ∇ and r, and adjust the network again. Then, we should examine the network adjustment results (Fig. 1.2) again. If the factor $1/\sigma^2$ of the zenith angles are better, but still the worst, we should repeat the process. If there is another component whose $1/\sigma^2$ is worst than zenith angles, such as direction sets, we should apply the process on this component.

In the end, we can reach the acceptable results after some iterations. The network adjustment results are shown in Fig. 1.4. If we check the measurements, we can find that some of them are enabled, but all of them fulfill the requirement, i.e. the highlights are green, see Fig. 1.5. The graphic and the coordinates of the local reference frame are shown in Fig. 1.6 and Table 1.1.

Pint-ID	East y [m]	North x [m]	Height z [m]	σ_y [mm]	σ_x [mm]	σ_z [mm]
FP1	-4.3985	54.2824	-2.1526	1.0	0.5	0.4
FP2	15.1293	8.3400	-1.7653	0.6	0.6	1.1
FP3	95.9545	28.1176	1.4638	0.9	0.7	0.5
FP4	67.5471	-7.8067	0.1150	0.6	0.8	0.4
FP5	15.1268	-31.8968	-1.3757	0.6	0.6	0.5
FP6	-2.0825	73.1537	-2.3326	0.9	0.7	0.5
FP7	41.2947	41.3393	-1.5025	1.0	0.7	0.5

Table 1.1: *The coordinates of the local network*

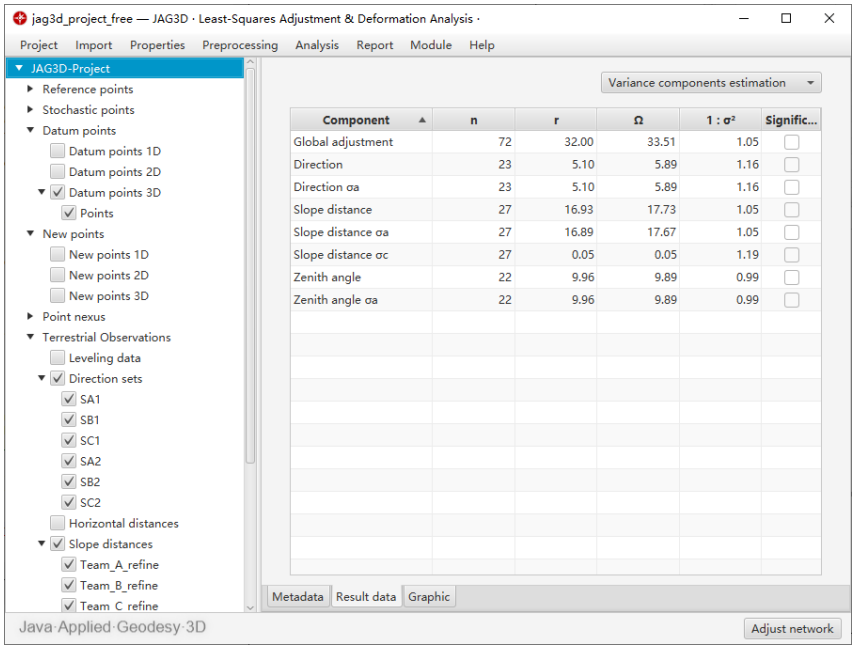

Figure 1.4: *The network adjustment results of the local network*

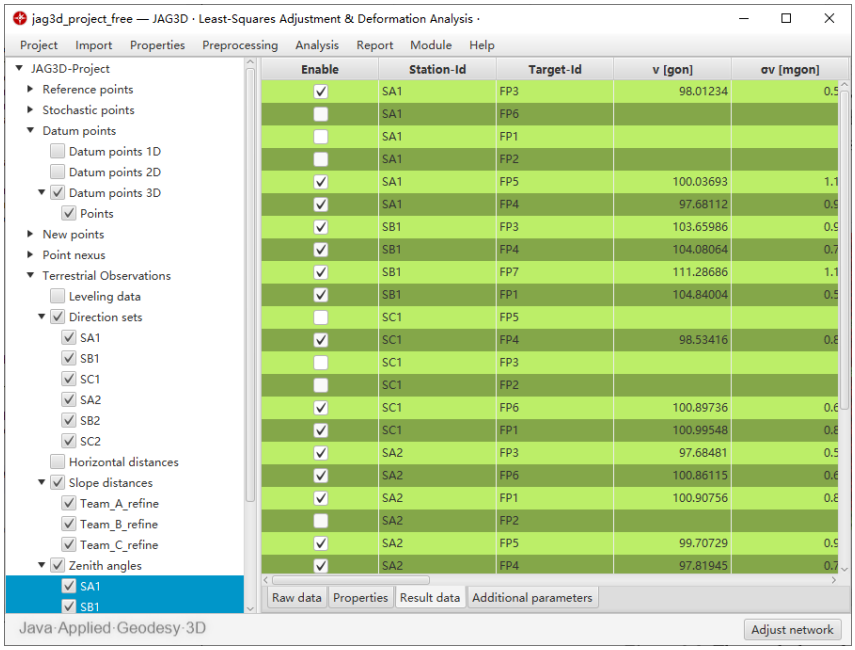

Figure 1.5: *The result data of zenith angles of the local network*

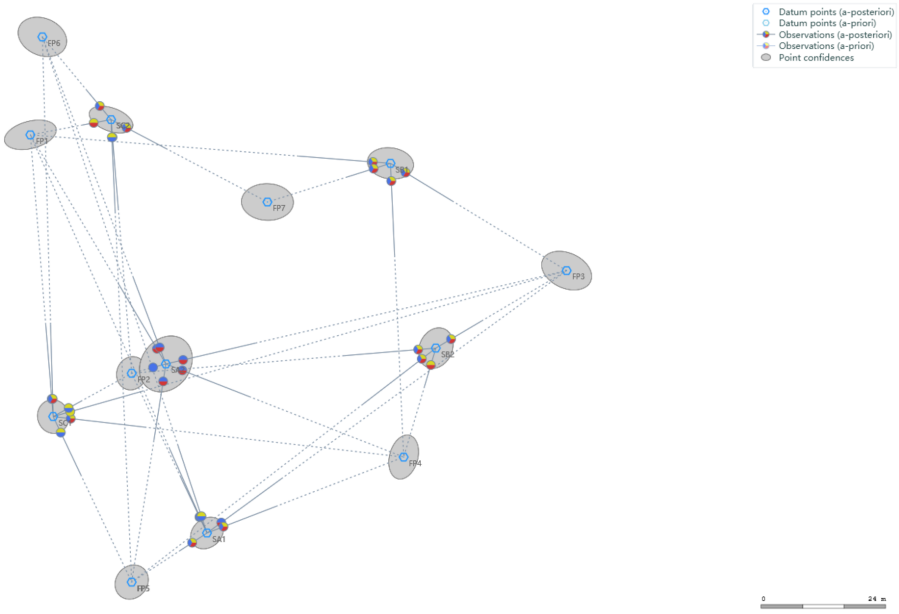

Figure 1.6: *The graphic of the local network*

1.3 The global network frame

When we have the results from the WP1 and WP3, i.e. the UTM coordinates and the DHHN heights of FP1 to FP3, we can solve the datum problem by using these information. In this step, we have tried to consider the FP1 to PF3 as stochastic points and reference points, but both of them were not successful, which means, the configuration of these three points from WP1 and from the local reference system do not mach to each other (see Table 1.3). The possible reason is: due to some operational errors in our field measurements, the UTM coordinates from the GNSS measurement still include some blunders. Therefore, we decided to consider FP1 to FP3 as datum points, which means the coordinates of these three points will also be changed during the adjustment. The other points are considered as new points.

The process is basically the same as described in Section 1.2. The only different is that the network adjustment was conducted with a part trace minimization (FP1 to FP3). The statistic parameters of the network adjustment results are shown in Fig. 1.7. The graphic and the coordinates of the global reference frame are shown in Fig. 1.8 and Table 1.2. The differences between the coordinates of WP2 and WP1 are shown in Table. 1.3. We can find, the maximal difference is already about 2.6 cm. And the biggest problem is by FP3.

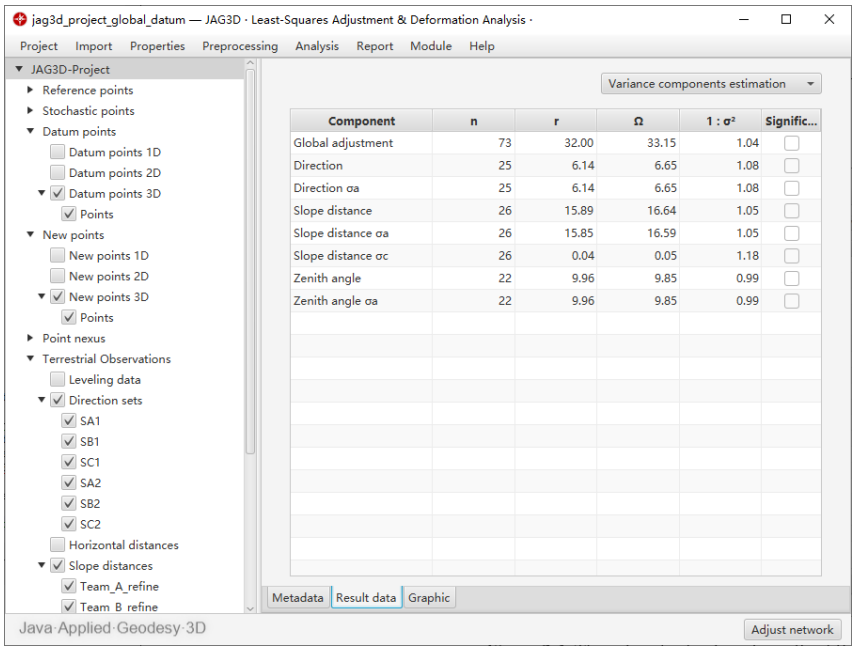

Figure 1.7: *The network adjustment results of the global network*

Point ID	East y [m]	North x [m]	Height z [m]	σ_y [mm]	σ_x [mm]	σ_z [mm]
FP1	32507095.3583	5398980.0529	454.3731	0.7	0.8	0.6
FP2	32507072.1621	5398935.8518	454.7604	0.7	0.8	0.8
FP3	32507140.5414	5398883.4873	457.9895	0.5	0.8	0.5
FP4	32507092.8496	5398885.0535	456.6407	1.1	0.8	0.6
FP5	32507041.0142	5398910.3787	455.1500	0.9	1.1	0.7
FP6	32507111.4344	5398990.2078	454.1932	1.2	1.1	0.7
FP7	32507114.2705	5398936.4895	455.0232	1.0	1.1	0.7

Table 1.2: *The coordinates of the global network*

Point ID	East y [m]	North x [m]	y (WP1) [m]	x (WP1) [m]	Δy	Δx
FP1	32507095.3583	5398980.0529	32507095.3659	5398980.0269	-0.0076	0.0260
FP2	32507072.1621	5398935.8518	32507072.1704	5398935.8519	-0.0083	-0.0001
FP3	32507140.5414	5398883.4873	32507140.5255	5398883.5132	0.0159	-0.0259

Table 1.3: *The differences between the coordinates from WP2 and WP1*

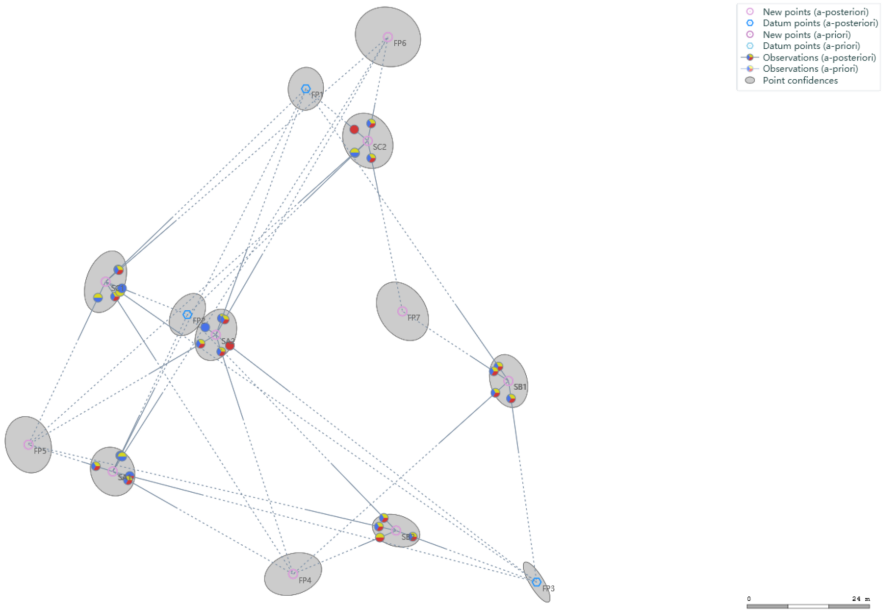

Figure 1.8: *The graphic of the global network*

1.4 Coordinates transformation

JAG3D also provides the coordinates transformation function, so we can easily transform the local coordinates of the checkpoints measured by Team D into the global network frame. The window of the transformation function is shown in Fig. 1.9. Since we have measured the slope distances, the scale are already determined. Therefore, a 6-parameter transformation has been chosen.

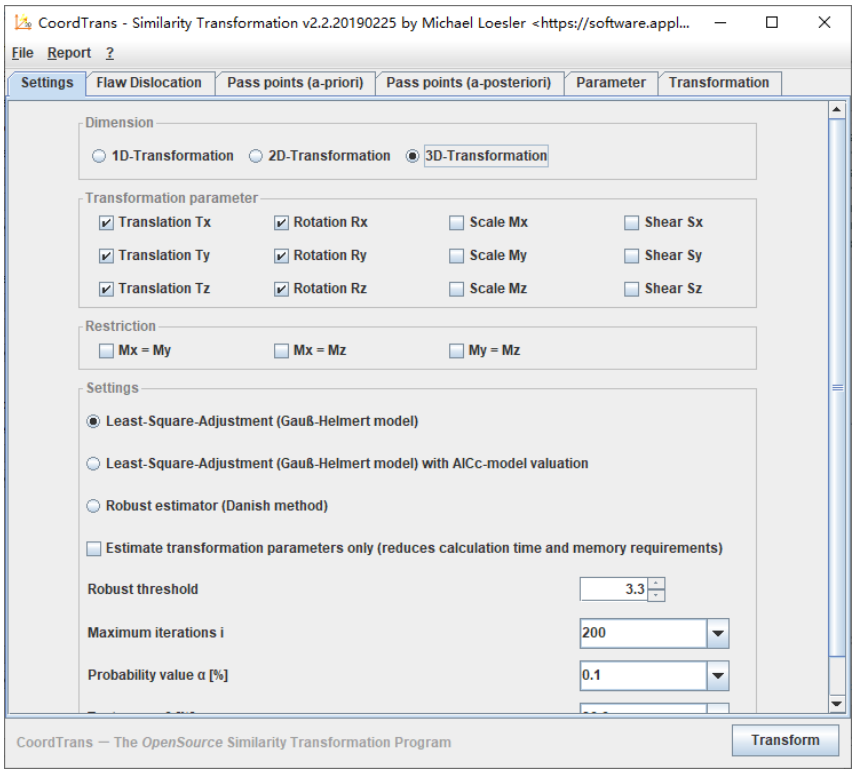

Figure 1.9: *The window of the transformation function*

The results are shown in Table 1.4.

Point ID	East y [m]	North x [m]	Height z [m]	σ_y [mm]	σ_x [mm]	σ_z [mm]
C1	32507114.1390	5398953.1817	456.5028	0.4	0.4	0.8
C2	32507133.1575	5398907.6819	459.8789	1.8	1.1	2.2
C3	32507117.9851	5398897.5838	456.9178	2.0	1.0	2.0
C4	32507092.4091	5398914.7301	458.2085	1.6	1.0	2.5
C7	32507080.0753	5398930.3924	456.5569	1.3	1.1	3.0
C9	32507118.8133	5398928.7297	456.9426	0.4	0.4	0.6

Table 1.4: *The global coordinates of the checkpoints*

1.5 Conclusion

In the WP2, we have used *Leica TS30* to measure the 3D network with free station points. Then, two network adjustments have been conducted with a complete and part trace minimization to build the local and global 3D geodetic network frame.

Although some problems occurred during the measurements of WP1 and WP2, which caused the final networks between these two WPs are not completely consistent, we still got a reliable 3D geodetic network frame with the UTM coordinates and the DHHN heights. Based on this network, we have also measured the 3D coordinates of the required checkpoints for the WP5.

Integrierted Fieldwork 2020

WP3: Precision Levelling

Dr.-Ing. Martin Metzner

Supervisor

Martin Wilczynski

Student

Carsten Helfert

Student

University of Stuttgart
Germany

Contents

1. Introduction

Work Package 3 is about delivering height information for other WPs. The goal was to deliver the heights with a standard deviation of σ_i < 1mm. Therefore, precision levelling was used. 3 routes were made starting and ending at a benchmark point with known height. In the first thoughts each route should be measured two times, as the circumstances only allowed us to measure it once, that's why a short route 3 was included.

2. Progress of the measurements

The leveling should take place on two days. Each Group consists of two Teams. On the first day route 1 and 2 should be measured. In the beginning we realized that your accuracy regarding back- and foresight $(B_1 - F_1) - (B_2 - F_2)$ < 0.05mm was too high. So, it got increased to < 0.1mm.

It took the first group around 7 hours instead of the planed 2 hours, meaning only one levelling could be done this day. This experience made us think about our plans, so we decided to measure each route once and include a new route from benchmark to benchmark. Thanks to our third measurement, a difference of 1.7mm has been found between the given heights of the benchmarks.

Here is the course of each route

- route 1: 5642 →FP3→FP2→FP1→FP2→FP3→5642
- route 2: 5641 →FP1→FP2→FP3→FP2→FP1→5641
- route 3: 5642 →5641→5642

3. Analysis of the measurements

The analysis is based on the data achieved from the measurements. The figures 2-3 below show the height differences and aim distances between the points of interests.

The routes got measured two times, once on the way there and the way back.

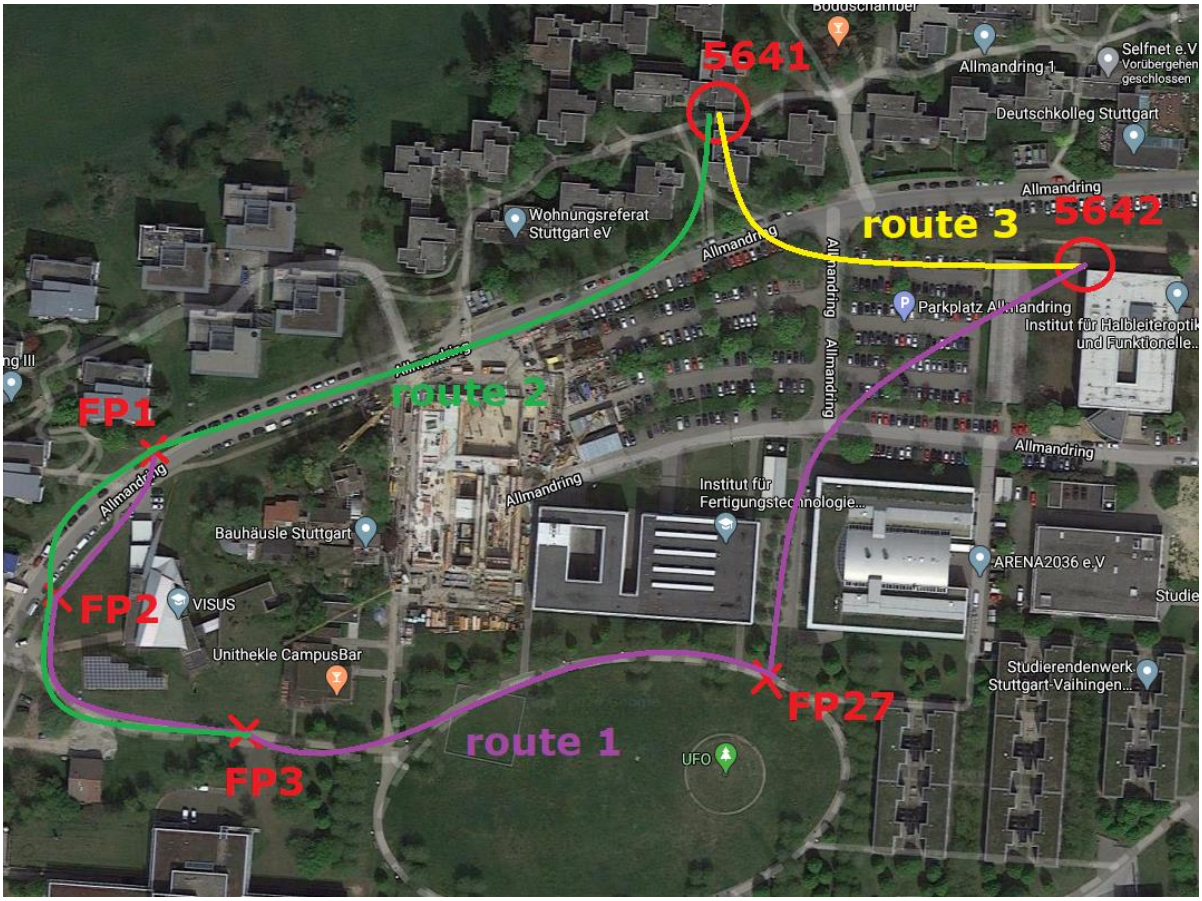

Figure 1 Configuration

First, we look at the heights of each route. The heights between the points of interest (in figure 2 and figure 3) are the same. The direction of each route is different that's why it's mirrored.

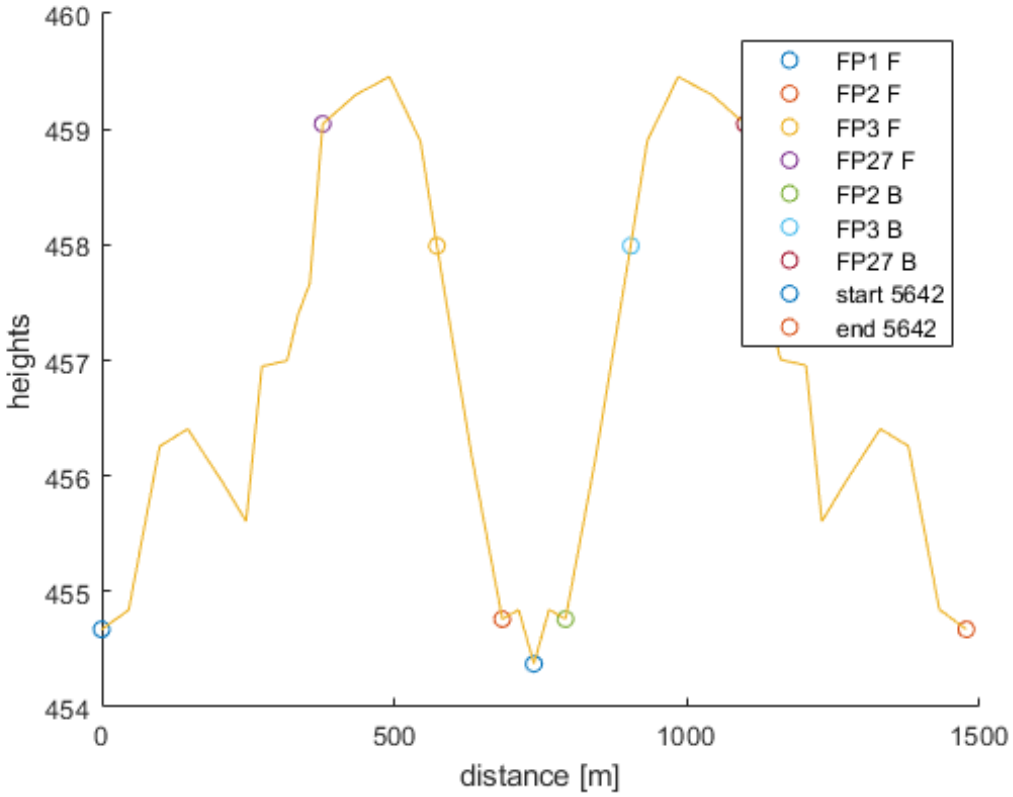

Figure 2: Heights of route 1

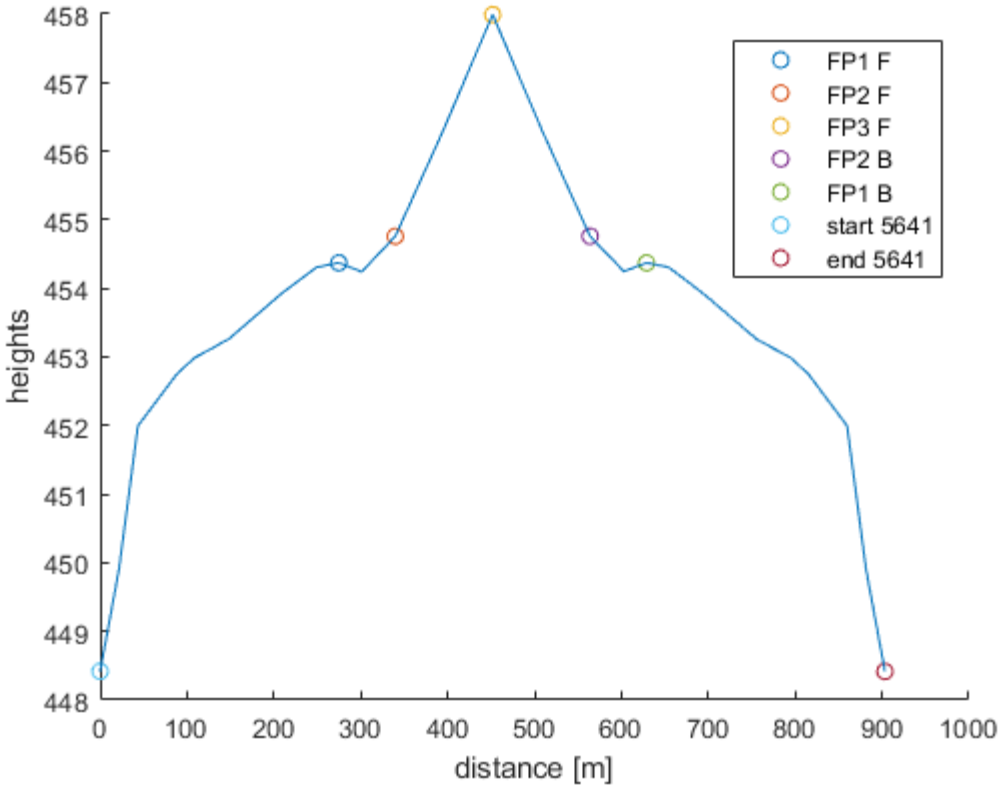

Figure 3: Heights of route 2

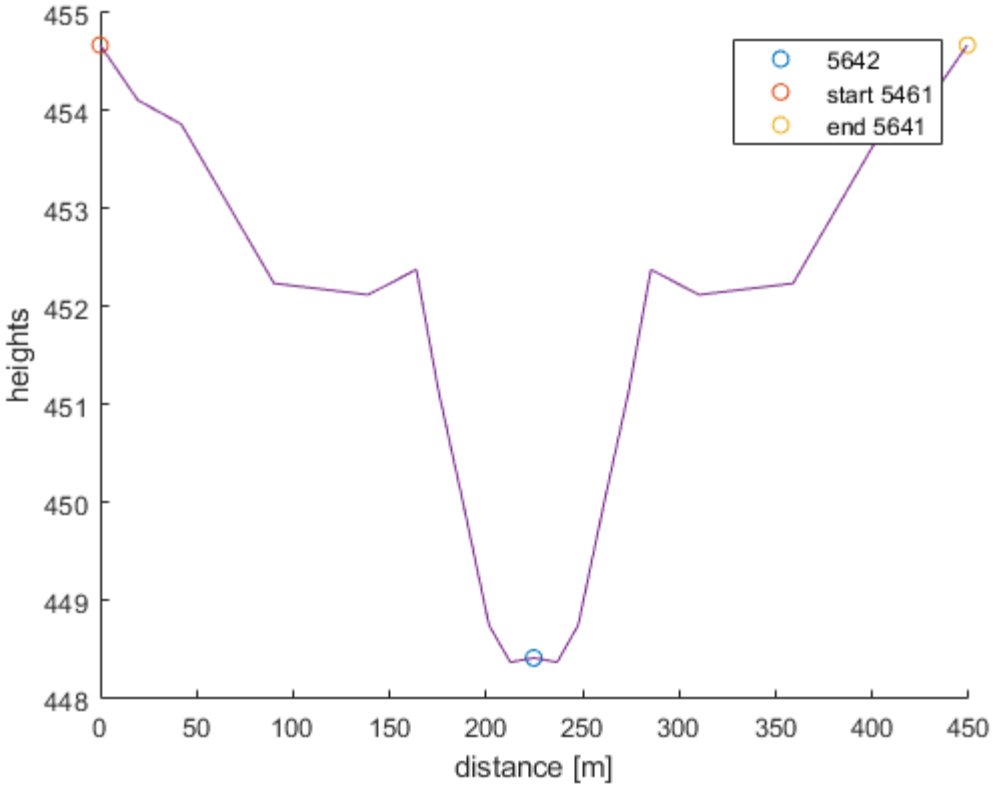

Figure 4: heights of route 3

One of the requirements is that the difference between the target distance should not be over 20cm in total. This turned out to be a problem when operating on terrain with big height differences or instrument positions where the target distance is big. The following figures 5-7 show all measurements, (accepted ones and the ones which didn't got accepted in the later work) and the difference in target distance. The orange line shows our required accuracy of 20cm, all measurements over this value had to be discarded and we had to position the instrument again. The yellow line is the standard setting for the Trimble Dini 0.3, which was used for the levelling. The value of 1m was found in the instructions of the instrument. As we see, the first group had to repeat a lot of measurements because of this error. For the later measurements a function was used, that can measure the distance to the levelling staff, that's why the later figures don't show this error anymore.

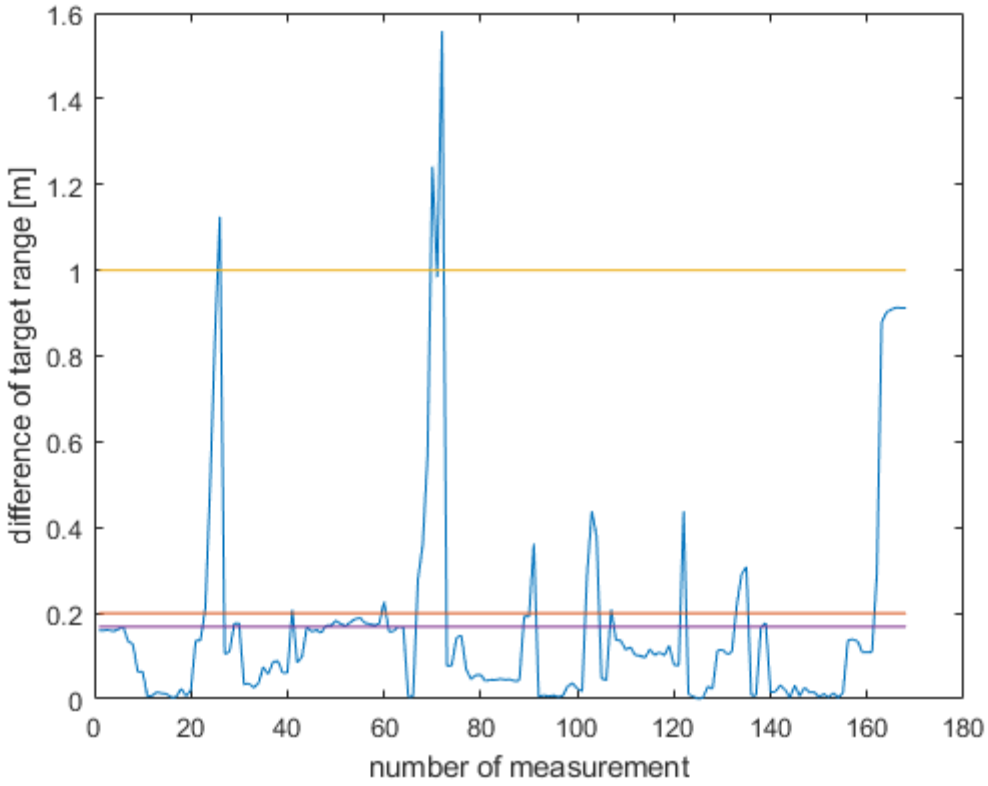

Figure 5: difference of target range route 1

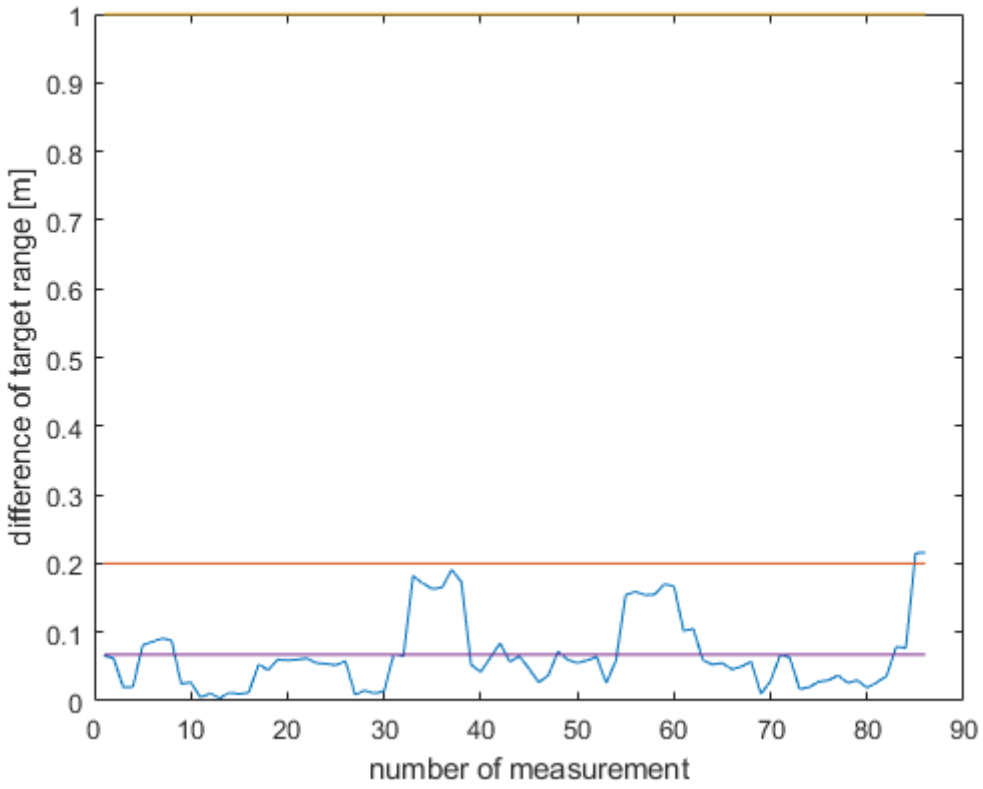

Figure 6: difference of target range route 2

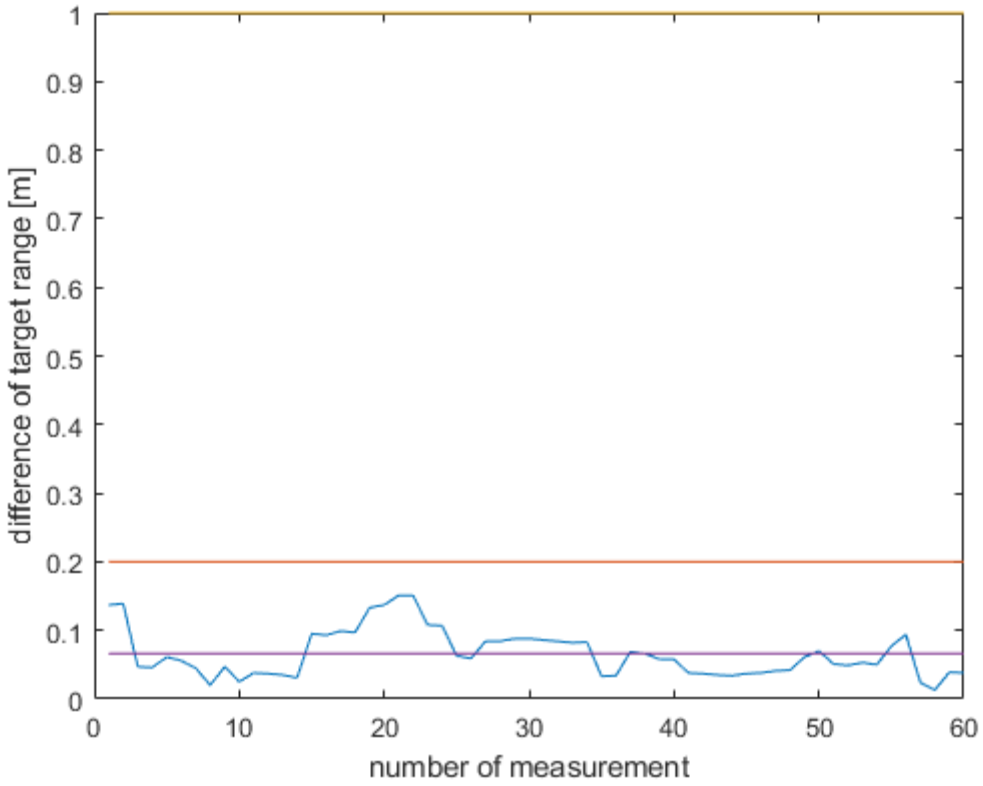

Figure 7: difference of target range route 1

As mentioned before the requirement of difference between fore- and back sight of < 0.05mm got increased up to <0.1mm. This requirement was the main reason in the latter two routes why measurements on certain instrument positions had to be repeated. As before the yellow line is, he standard setting for the Dini and the purple line is the average. Following figures 8-10 show this type of error:

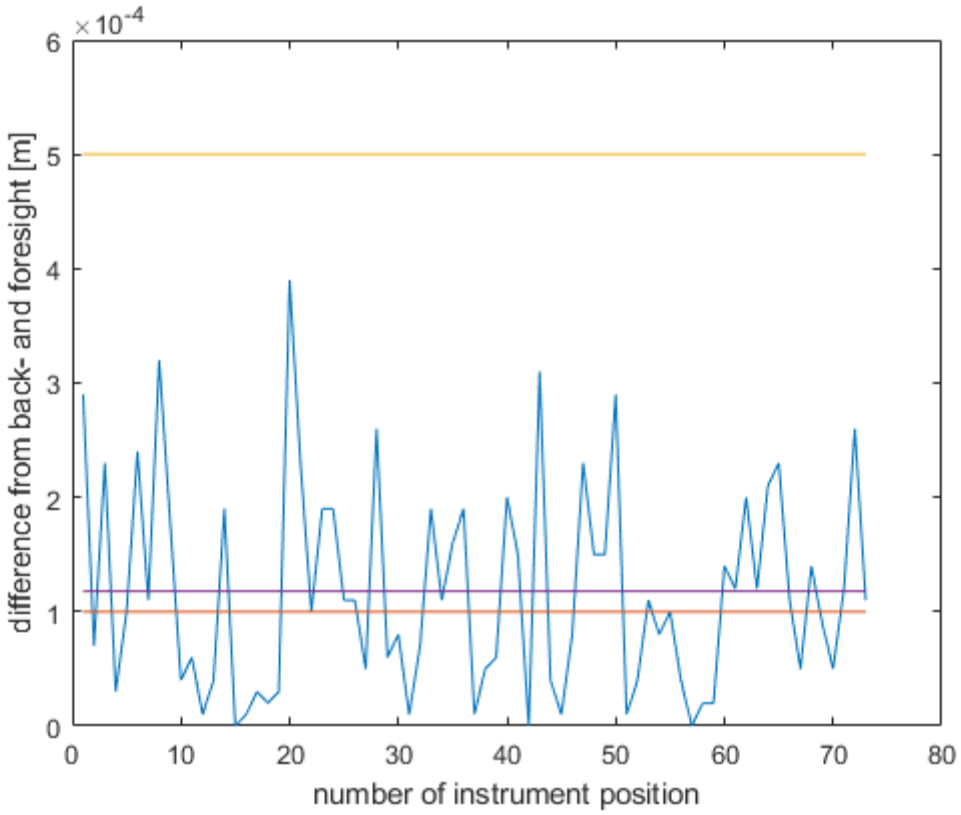

Figure 8: difference B1F1 and B2F2 route 1

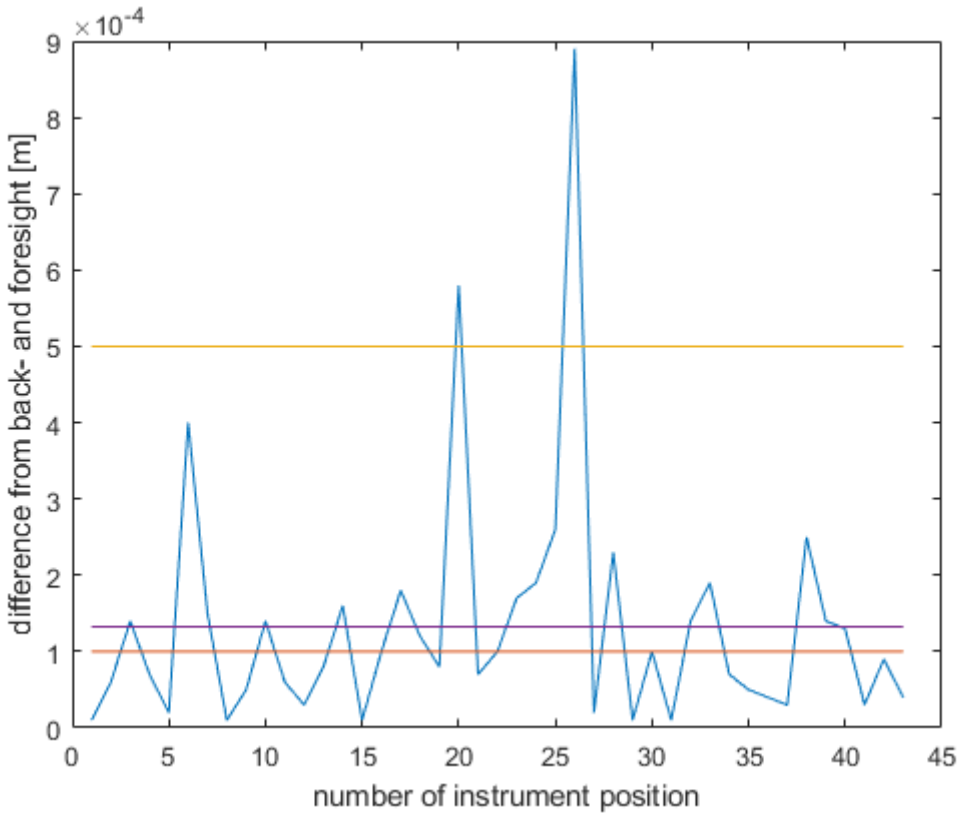

figure 9 difference B1F1 and B2F2 route 2

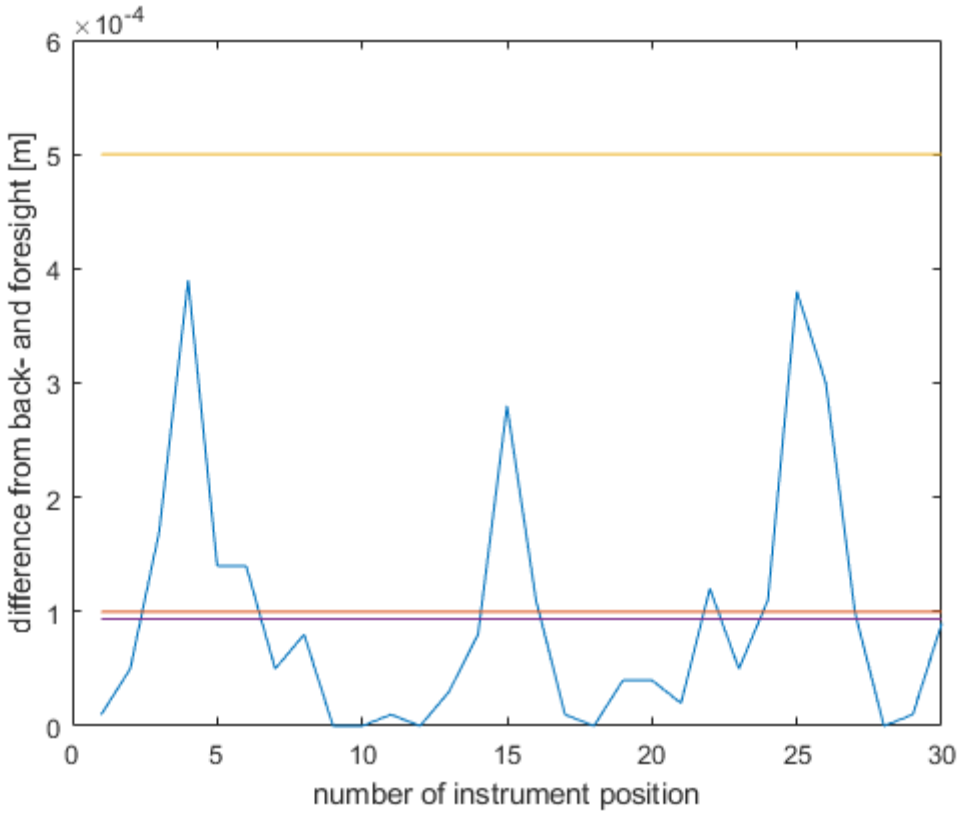

Figure 10: difference B1F1 and B2F2 route 3

It's up to the required accuracy to decide for a fitting limitation. This requirement cost the measurement groups a lot of time.

4. Adjustment

A conditionally adjustment (B-Model) was made. Conditional equations were made that the same heights differences from point to point should be equal. A route between the benchmarks was made, so the benchmarks aren't seen as flawless and are also taken in our adjustment.

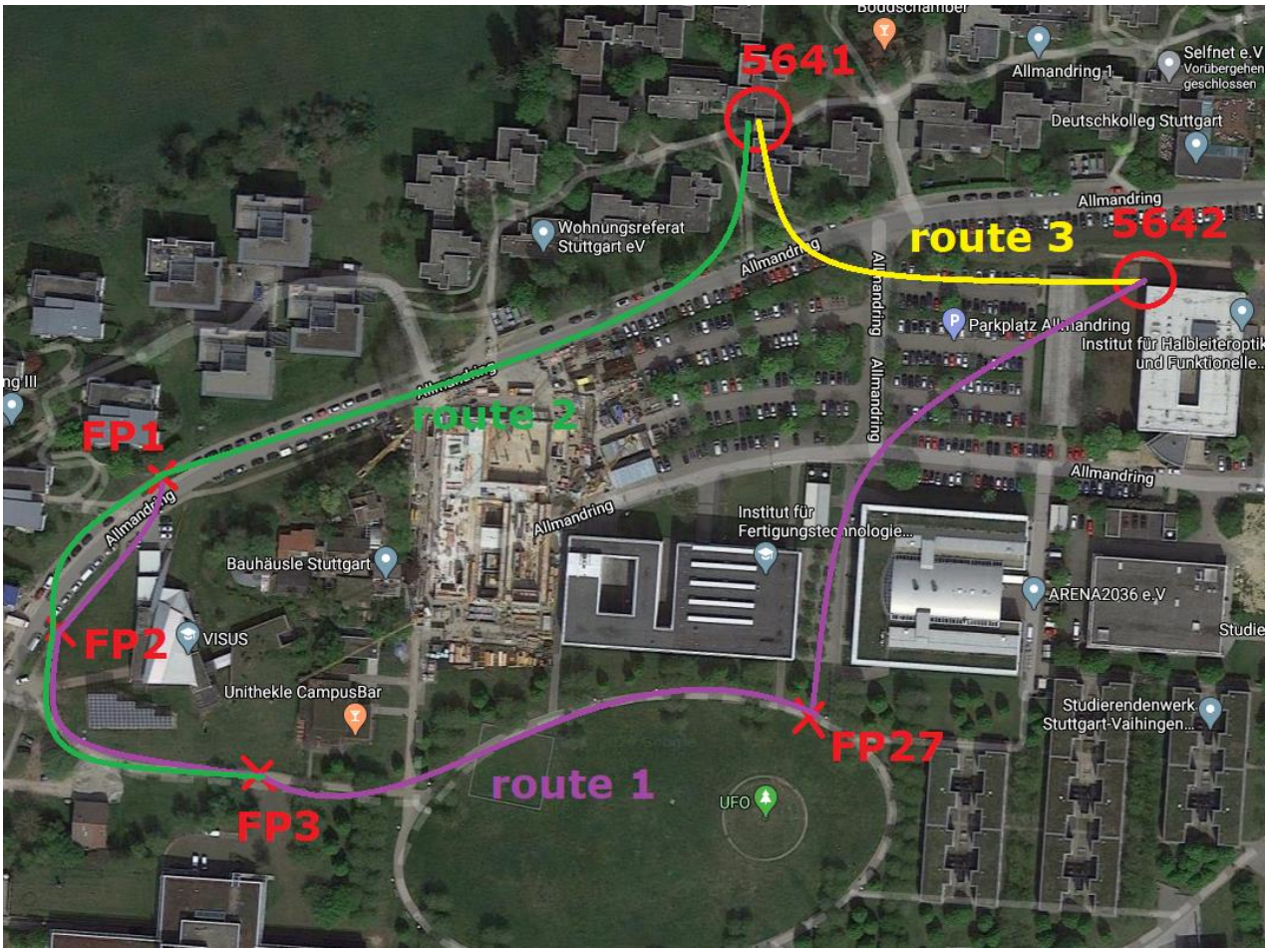

Figure 11: Configuration

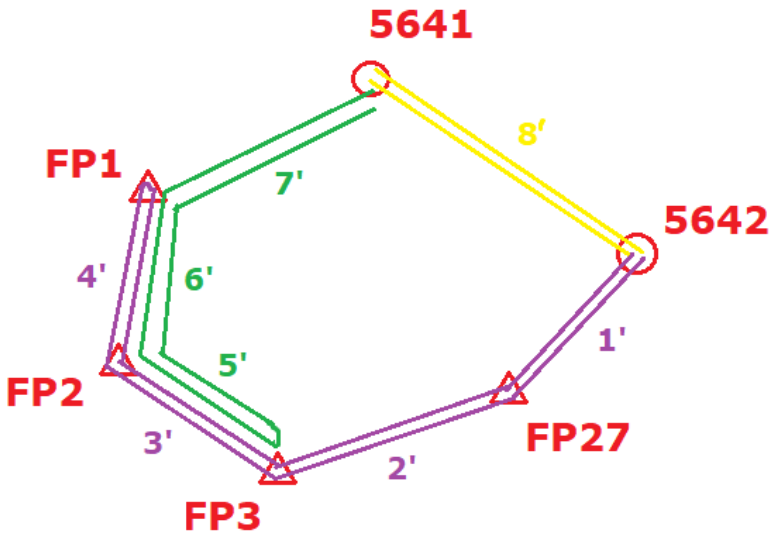

Figure 12: simplified configuration

The measurements in our configuration are made clockwise. Meaning for example the path 8’ is made from benchmark 5641 to 5642. 8’’ would be counterclockwise. Therefor we get following matrices for our B-Modell:

$$B = \begin{bmatrix} 1 & 1 & 0 & 0 & 0 & 0 & 0 & 0 & 0 & 0 & 0 & 0 & 0 & 0 & 0 & 0 & 0 & 0 \\ 0 & 0 & 1 & 1 & 0 & 0 & 0 & 0 & 0 & 0 & 0 & 0 & 0 & 0 & 0 & 0 & 0 & 0 \\ 0 & 0 & 0 & 0 & 1 & 1 & 0 & 0 & 0 & 0 & 0 & 0 & 0 & 0 & 0 & 0 & 0 & 0 \\ 0 & 0 & 0 & 0 & 0 & 0 & 1 & 1 & 0 & 0 & 0 & 0 & 0 & 0 & 0 & 0 & 0 & 0 \\ 0 & 0 & 0 & 0 & 0 & 0 & 0 & 0 & 1 & 1 & 0 & 0 & 0 & 0 & 0 & 0 & 0 & 0 \\ 0 & 0 & 0 & 0 & 0 & 0 & 0 & 0 & 0 & 0 & 1 & 1 & 0 & 0 & 0 & 0 & 0 & 0 \\ 0 & 0 & 0 & 0 & 0 & 0 & 0 & 0 & 0 & 0 & 0 & 0 & 1 & 1 & 0 & 0 & 0 & 0 \\ 0 & 0 & 0 & 0 & 0 & 0 & 0 & 0 & 0 & 0 & 0 & 0 & 0 & 0 & 1 & 1 & 0 & 0 \\ 0 & 0 & 0 & 0 & 1 & 0 & 0 & 0 & 0 & 1 & 0 & 0 & 0 & 0 & 0 & 0 & 0 & 0 \\ 0 & 0 & 0 & 0 & 0 & 0 & 1 & 0 & 0 & 0 & 0 & 1 & 0 & 0 & 0 & 0 & 0 & 0 \\ 1 & 0 & 1 & 0 & 1 & 0 & 1 & 0 & 0 & 0 & 0 & 0 & 1 & 0 & 0 & 0 & -1 & 1 \\ 0 & 0 & 0 & 0 & 0 & 0 & 0 & 0 & 0 & 0 & 0 & 0 & 0 & 0 & 1 & 0 & 1 & -1 \end{bmatrix} \quad y = \begin{bmatrix} \Delta H_{1'} \\ \Delta H_{1''} \\ \Delta H_{2'} \\ \Delta H_{2''} \\ \Delta H_{3'} \\ \Delta H_{3''} \\ \Delta H_{4'} \\ \Delta H_{4''} \\ \Delta H_{5'} \\ \Delta H_{5''} \\ \Delta H_{6'} \\ \Delta H_{6''} \\ \Delta H_{7'} \\ \Delta H_{7''} \\ \Delta H_{8'} \\ \Delta H_{8''} \\ H_{5641} \\ H_{5642} \end{bmatrix}$$

The adjustment is weighted. With focus on the aim ranges. The benchmarks are seen the most accurate while the shorter paths more accurate then paths with longer distances. The length of a path was calculated trough addition of the target distances between instrument positions.

5. Results

We estimated the heights of four points of interests. Three of the points (FP1, FP2, and FP3) are in the measurement area around the VISUS-building. The points are circled in red in the following figure 12. These heights are of interest for WP2 and WP5.

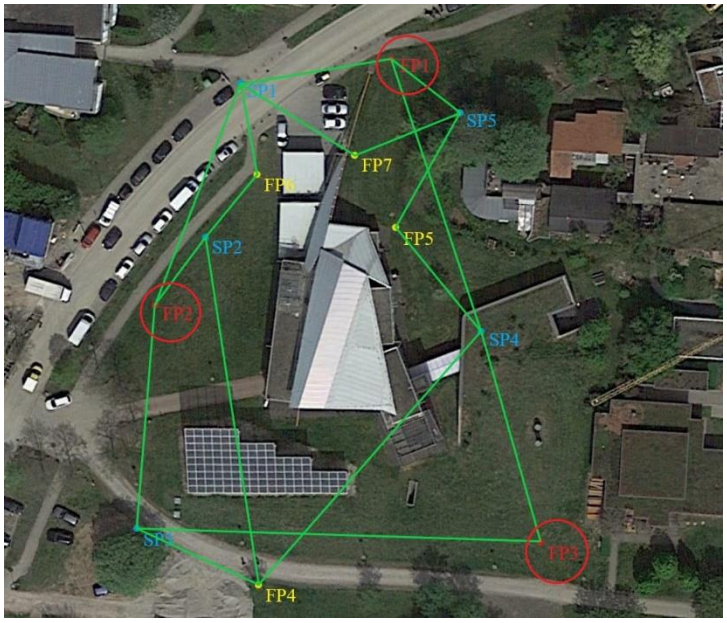

Figure 12: measurement area around the VISUS building

FP27 was of interest for WP4, that's why it also got estimated.

Point of interest	heights (NHN) [m]	Standard deviation [mm]
FP 1	454,3731	0,98
FP 2	454,7596	0,95
FP 3	457,9903	0,87
FP 27	459,0454	0,7

Integrated Fieldwork 2020

WP4: Navigation Routes/Paths near Hysolar

Supervisors

Clemens Sonnleitner

Students

Torben Blei

University of Stuttgart
Germany

Contents

1. Introduction

In this WP, the height profile of the area of the Integrated Field Work will be measured by using GNSS in a kinematic survey. For reaching a high precision, Real-Time-Kinematic (RTK) will be applied.

A remote-controlled car will be used as foundation for the rover. A mobile multi-band RTK GNSS receiver is installed on top of the car, which then allows kinematic surveying. A multiband RTK reference GNSS station positioned at a reference point, which provides good Satellite-visibility in terms of Multipath and is located near the middle of the area of interest will then provide correction data.

Piloting the car along the edges of defined roads creates the desired raw data which, together with the correction data, can later be used within the post-processing to create RTK positions using RTKlib.

2. Objectives

The main objective of this project is to create three-dimensional trajectories of the chosen roads in local ETRS89-UTM coordinates.

The second objective is to give a general view on the accuracy that can be achieved using RTK measurements and their benefits compared with single-point-positioning.

3. Preparations

Then the settings of the rover need to be set. As the project will be using GNSS in a kinematic survey, the rovers positioning mode needs to be kinematic. Afterwards, a scanning rate of 10 Hz is sufficient. Raw data and Base correction both will be logged in RINEX 3.03, the Position in ENU System.

The settings of the reference station are dependent on the settings chosen for the rover as the logging if the output files should be similar. The same does account for the scanning rate.

In the next step the roads of interest must be chosen. Therefore, they need to be checked in terms of passability and reachability from the base station and the router, depending on the chosen way of transmitting.

As a last step, a coordinate transformation tool needs to be chosen or created to transform WGS84 into ETRS89-UTM coordinates.

4. Field Plan

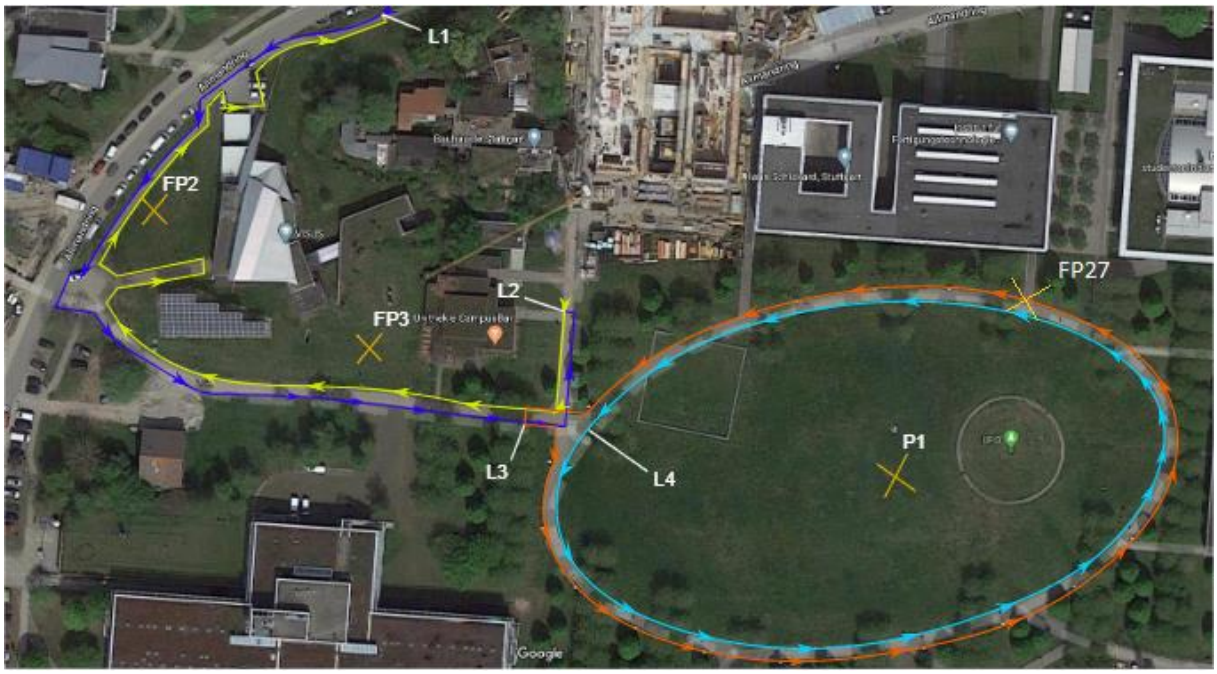

Figure 1: Field Plan with Routes and Points

Group	Routes
Group A	1. L1 – L2: purple (path 1) 2. L2 – L1: yellow (path 2)
Group B	1. L1 – L2: purple (path 1) 2. L2 – L1: yellow (path 2)
Group C	1. L3 – L3: orange (path 3) 2. L4 – L4: blue (path 4)
Group D	1. L3 – L3: orange (path 3) 2. L4 – L4: blue (path 4)

Table 1: Route division

5. Process

During the fieldwork, all groups followed the implementation correctly which can be seen in the good labelling of the data files, as well as in the similar quality between the data itself.

During the measurement drives alongside the designated routes, all groups were facing only smaller problems, like unclear edges of the roads which were used as orientation for the driver or too tight curves within the road at which the car had to be turned around by hand. Even though those problems led to some irritations they were solved in a similar way, which is why the data can be used.

6. Post Processing

On behalf of the post processing the raw data from the base station and the rover were used to calculate the RINEX observation and navigation files in RTKconv as the internal conversion didn't include all frequencies. Subsequently these files were turned into kinematic position solutions using RTKpost. Therefore, the exact base station coordinates from the different groups where needed as well as the antenna height of the rover. Both have been measured by the groups:

Groupe	lat [deg]	lon [deg]	h [m]	Rh [cm]
A	48.74279667	9.09911231	510.407	28.0
B	48.74279286	9.09911954	510.440	28.0
C	48.74280263	9.09912009	510.346	28.3
D	48.7427910	9.09906902	510.436	28.0

Table 2: base station coordinates in latitude (lat), longitude (lon) and height (h) (WGS84) as well as antenna heights from the rover over the ground (Rh)

During the calculations in RTKpost the results have been checked for errors. Using all Satellite systems including BEIDOU and GALLILEO the results were bad concerning fixed solutions:

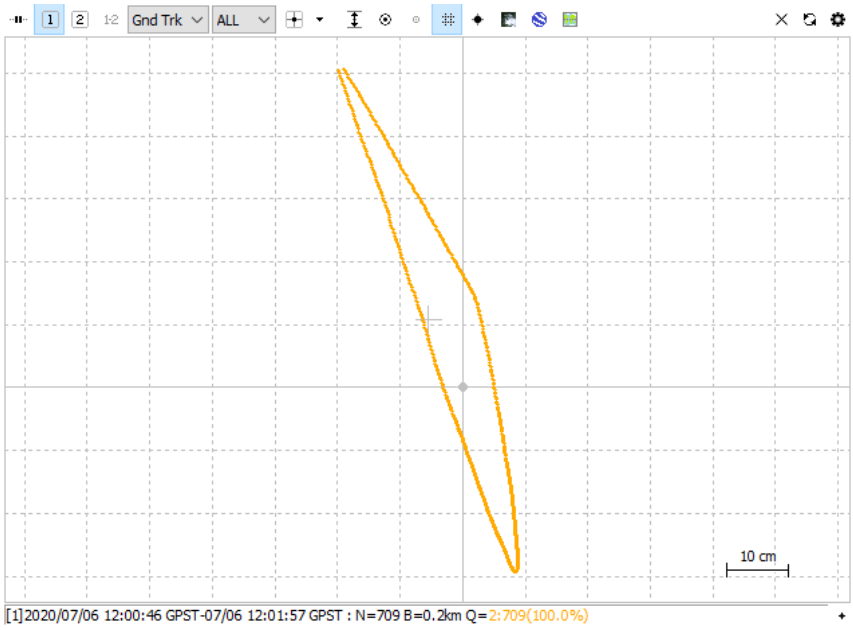

Figure 2: rover measurements FP2 from Team A using all satellites

As can be seen in Figure 2 the rover position changes significantly during the one minute of measurements. These variations of more than 80 cm without rover movement are indicated by the solution status which shows 100% of float solutions (yellow). This problem was solved by changing the satellite systems used in the calculations:

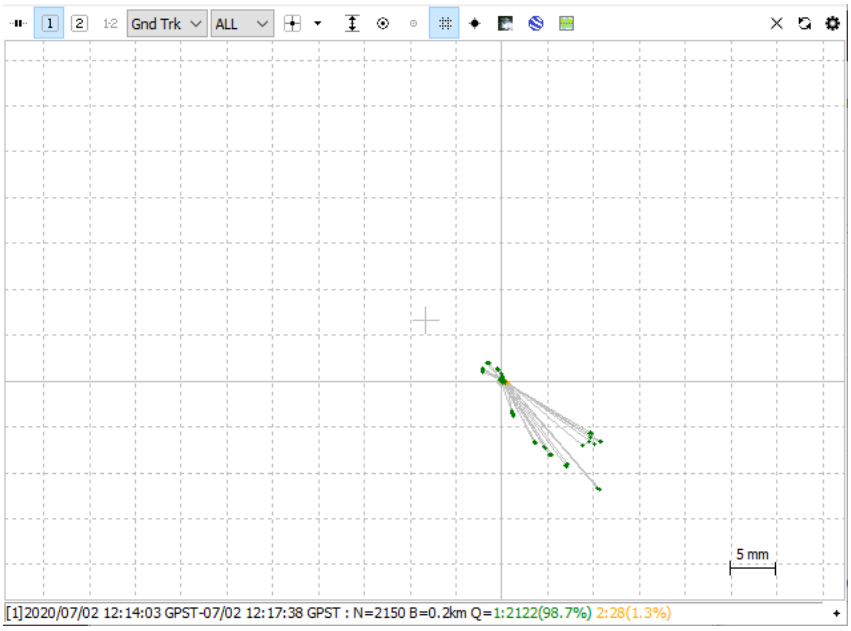

Figure 3: rover measurements FP2 from Team A using GPS and GLONASS

By disabling all satellite systems except GPS and GLONASS much better results were achieved (Figure 3). This is shown through the solution status showing 98.7% fixed solutions (green).

The satellite systems used for the calculations of the static points and the kinematic routes were chosen as:

- Static points: GPS and GLONASS
- Kinematic routes: GPS and GLONASS

7. Analysis and results

Analysis of static points FP2, FP3 and FP27:

Point	Group	Y [m]	X [m]	h [m]	dY [m]	dX [m]	dh [m]
FP2	WP 2	32507072.162	5398935.851	454.760	-	-	-
	A	32507072.166	5398936.796	454.895	0.005	-0.055	0.135
	B	32507072.123	5398938.815	454.892	-0.038	-0.035	0.132
	C	32507072.192	5398935.577	454.836	0.030	0.006	0.075
	D	32507071.155	5398936.821	454.821	-0.006	-0.030	0.060
FP3	WP 2	32507140.541	5398883.487	457.989	-		-
	A	32507140.420	5398883.491	457.578	-0.140	-0.005	-0.098
	C	32507140.828	5398884.297	458.055	0.007	0.022	0.065
	D	32507139.870	5398883.970	458.044	-0.021	0.026	0.055
FP27	WP3	-	-	459.045	-	-	-
	A	-	-	460.126	-	-	1.080
	B	-	-	459.842	-	-	0.797
	C	-	-	458.599	-	-	-0.447
	D	-	-	458.661	-	-	-0.384

Table 3: averaged coordinates of FP, FP3 and FP27, compared with the results from WP2 and WP3 in UTM

While from FP27 only the height was measured by WP3, FP2 and FP3 both have been measured by WP2 including UTM coordinates. By comparing the results between WP2 and WP3 with the measurements from WP4 the accuracy of the RTK measurements of the rover can be checked. Therefore, averaged coordinates will be needed as each static point has been measured for approximately 3 minutes. Also, the coordinates must be transformed into UTM as they are being calculated in geographic coordinates. The height must be transformed into orthometric height as it was measured in ellipsoidal height.

The height of the point FP27 shows significantly higher deviations compared with WP3 than the points FP2 and FP3 who were compared with WP2. This is caused by the different environmental conditions, as FP27 is covered by trees while the other points are not. This leads to differences in the solution status, as it changes from mostly integer (Q=1) to mostly float (Q=2) solutions:

Point	**Group**	**integer**	**float**	**Point**	**Group**	**integer**	**float**	**Point**	**Group**	**integer**	**float**
FP2	A	88.7%	11.3%	FP3	A	22%	78%	FP27	A	0%	100%
	B	65.7%	34.3%		B	-	-		B	0%	100%
	C	28.8%	71.2%		C	62.5%	37.5%		C	1.5%	98.5%
	D	98.7%	1.3%		D	52.9%	47.1%		D	-	-

Table 4: solution status of FP2, FP3 and FP27

As can be seen in table 3 the solution status of the groups A, B and C differs significantly between the points FP2, FP3 and FP27. Even though the points FP2 and FP3 have better results than FP27 some float solutions remain. They are caused by the high reflective Hysolar building.

To apply a control to the results given in Table 3 the differences of the averaged heights of the static points themselves between WP3 and WP4 were calculated:

Groupe	**FP2- FP3 [m]**	**FP2- FP27 [m]**	**FP3- FP27 [m]**
WP3	3.230	4.285	1.055
WP4	3.136	4.446	1.310
dh [m]	0.094	-0.161	-0.255

Table 5: height differences between the points FP2, FP3 and FP27 compared with WP3

As can be seen in table 4 the height differences between the points themselves confirm the accuracy given by the results in Table 3.

Kinematic measurements:

In addition to the static point measurements the paths near the high solar building were measured in a kinematic way:

Figure 4: purple and yellow routes measured by Group A

Figure 5: orange and blue paths measured by Groups C and D

The results of the best measurements combined create a nice relief, shown in Figures 4 and 5. As can be seen in those pictures, the measurement drives were affected by different environmental conditions like trees, covering the path or high reflective buildings. These cause the loss of the integer ambiguities, only float solution is available.

Figure 6: orange routes from Groups C (purple) and D (white)

Figure 6 shows those situations. The irregularities in the positions caused by trees is clearly visible.

Even tough Figure 6 shows some irregularities in context with high reflective buildings, they are best to be seen near the Hysolar building and adjacent solar panel:

Figure 7: yellow route from Group A in front of the Hysolar building

Measurements around the solar panel:

Additionally, a test drive was performed near the solar panel. The route taken by the rover was chosen randomly across the area of interest:

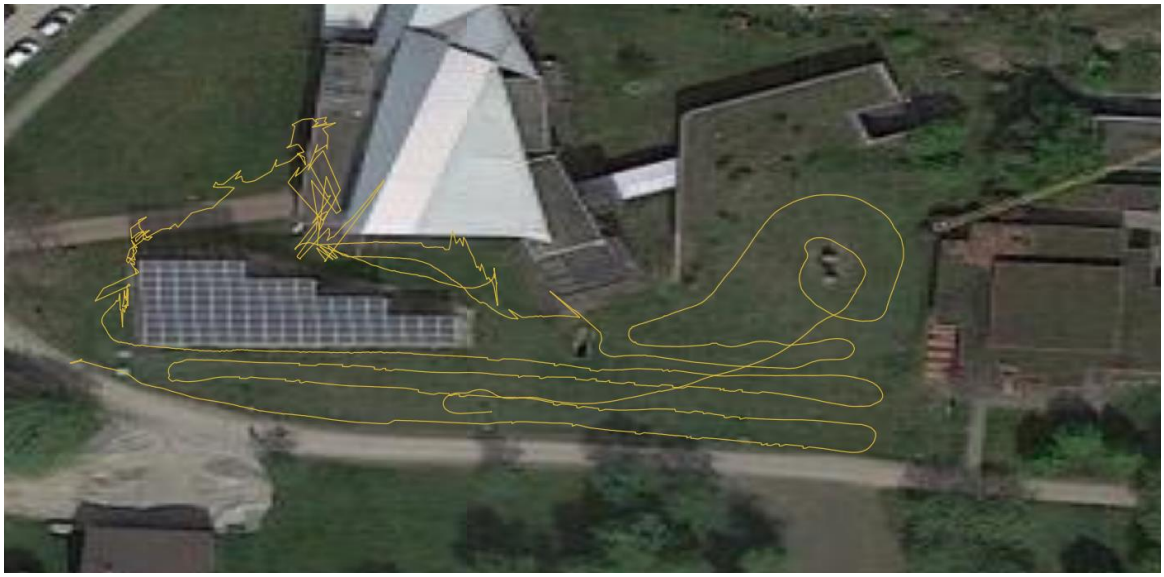

Figure 8: route around solar panel measured by Groupe B

The measured data allowed the creation of a height model of the area shown in Figure 8:

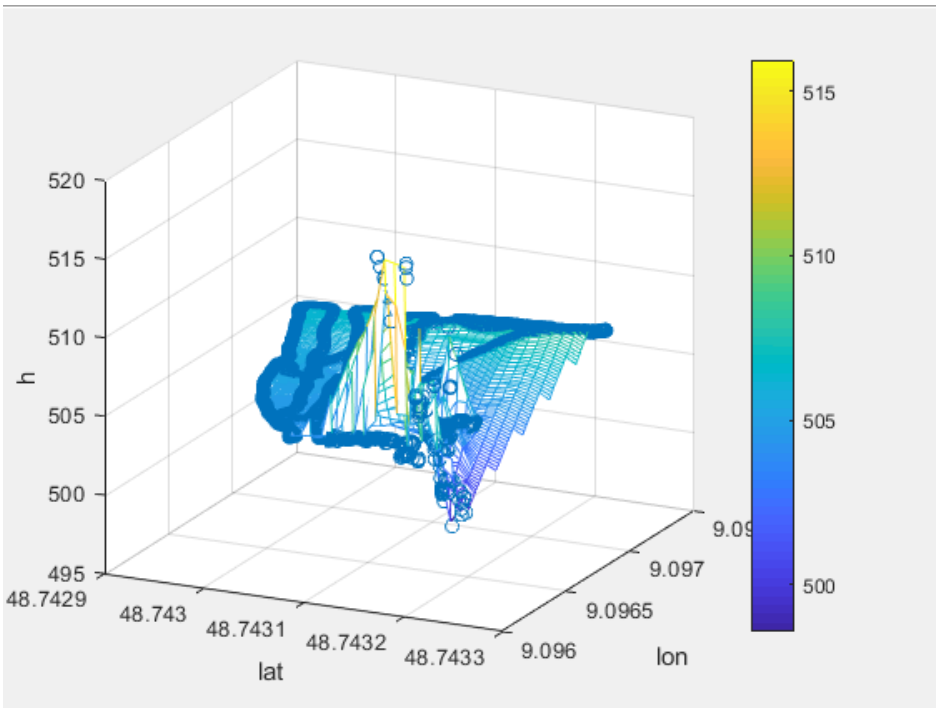

Figure 9: height model of Figure 8 as 3D image

As can be seen in Figure 9, the solar panel causes irregularities in the height. Those effects can be deleted by filtering out measurements with a float solution status:

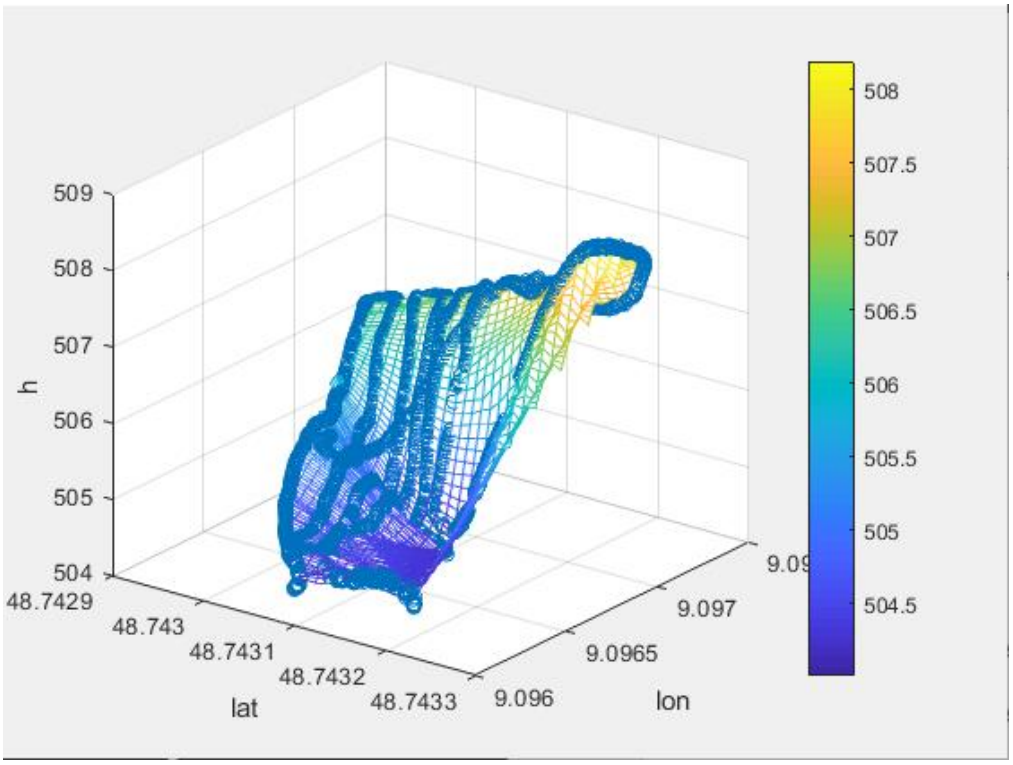

Figure 10: corrected height model of Figure 8 as 3D image

8. Conclusion

The analysis of the kinematic measurements can be used to create a fast overview over paths and roads if the accuracy fits the needed requirements. However different environmental conditions caused by trees or high reflective buildings should be taken in account. In these cases, additional measurement systems like inertial navigation sensors can be applied to minimize noise and create a more accurate movement pattern.

9. Sources

All map-based Figures were created with google maps: https://www.google.de/maps

Integrated Fieldwork 2020

WP5: Complementary 3D Object Reconstruction using Close-range Photogrammetry and Terrestrial Laser Scanning

Supervisors: N. Haala
M. Cramer
M. Kölle
P. Schneider

Students: Roman Geiger
Tim Kayser

University of Stuttgart
Germany

Contents

1. Introduction

In this work package, a terrestrial laser scanner, as well as a UAV-based camera system, were used to reconstruct a digital 3D model of the HySolar-Building. With the terrestrial laser scanner, data was collected by Light Detection and Ranging (LiDAR), while the UAV captured RTK-referenced Stereo-Images. Both methods were deployed from multiple viewpoints, to create and compare complete point clouds of the building.

2. Processing

UAV

The stereo pictures obtained by the UAV based camera system were processed using Agisoft's Metahsape software. Six checkerboard targets, of which the exact coordinates were determined by WP2, were used as ground truth information. Henceforth, after aligning the cameras, they were measured in each individual image. For the final alignment, we decided on the configuration shown below in figure 1, with four checkerboards as control points and two as check points. The final total error for the camera positions, control points and check points were all below 2 cm which was the approximate GSD used for the flights.

Cameras	Easting (m)	Northing (m)	Altitude (m)	Accuracy (m)	Error (m)
100_01...	507139.598790	5398933.835106	487.257759	**0.01139/0.01...**	0.006003
100_01...	507139.576846	5398939.837742	487.248759	**0.01117/0.01...**	0.006471
100_01...	507139.387655	5398945.676512	487.294759	**0.01095/0.01...**	0.007750
100_01...	507139.488409	5398951.546529	487.260759	**0.0113/0.011...**	0.015178
100_01...	507139.535839	5398957.595571	487.257759	**0.01108/0.01...**	0.010269
100_01...	507139.720329	5398963.459519	487.260759	**0.01139/0.01...**	0.011528
100_01...	507139.821000	5398969.394380	487.269759	**0.01107/0.01...**	0.020562
100_01...	507139.801307	5398975.233367	487.283759	**0.01137/0.01...**	0.018971
Total Error					**0.015872**

Markers	Easting (m)	Northing (m)	Altitude (m)	Accuracy (m)	Error (m)
C1	507114.139000	5398953.181700	456.502800	**0.0004/0.0008**	0.001326
C2	507133.157500	5398907.681900	459.878900	**0.0018/0.001...**	0.005493
C3	507117.985100	5398897.583800	456.917800	**0.002/0.001/0...**	0.006029
C4	507092.409100	5398914.730100	458.208500	**0.0016/0.001/...**	0.009706
C7	507080.075300	5398930.392400	456.556900	**0.0013/0.001...**	0.004583
C9	507118.813300	5398928.729700	456.942600	**0.0004/0.0006**	0.014359
Total Error					
Control points					0.004725
Check points					0.012255

Figure 1 - Metashape Alignment Configuration

We then calculated a dense point cloud, shown in figure 2, as well as a mesh, shown in figure 3, for this configuration.

Figure 2 - Dense Point Cloud from Metashape

Figure 3 - Mesh from Metashape

Problems

When aligning the cameras with the check points, we noticed a constant offset of about 18 cm along the positive y-axis, i.e. north, for all camera positions, which we corrected for the final alignment. This might have been caused by rounding errors when entering the RTK base stations position, which is used for correcting atmospherical effects on the measured GNSS signals and therefore impacts all measured projection centers equally.

Terrestrial Laser Scanner

The scans of the LiDAR sensor were processed using Cyclone, where the checkerboard coordinates received from WP2 were again used as control points for georeferencing. Furthermore, sphere targets were used as relative reference between the scans from multiple scan positions. The two setups of checkerboards and spheres used on the two days of measurement are shown in figure 4 and 5.

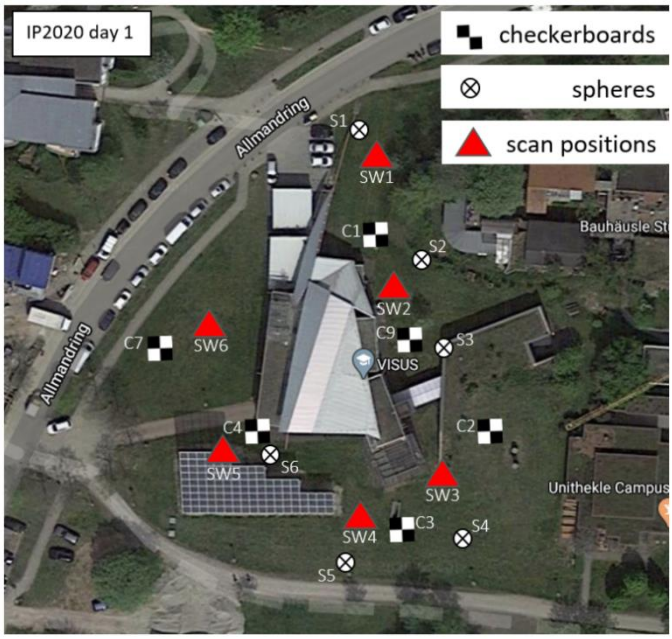

Figure 4 - Sketch of the Marker Setup for Day 1

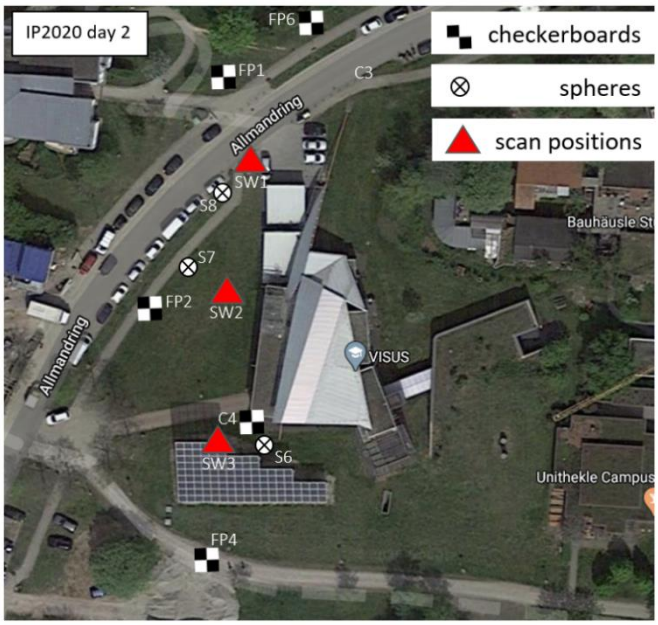

Figure 5 – Sketch of the Marker Setup for Day 2

As no total station measurements were planned for the second day, the checkerboards

were centred and levelled for fixed points (FP1, FP2, FP4, FP6), in order to use them as control points.

After correcting minor errors, such as incorrect target naming, the targets that the scanner did not automatically detect were measured manually/semi automatically in Cyclone, using high resolution target scans.

To geo-reference the registered point clouds we used the UTM-coordinates of the checkerboards measured by WP2.

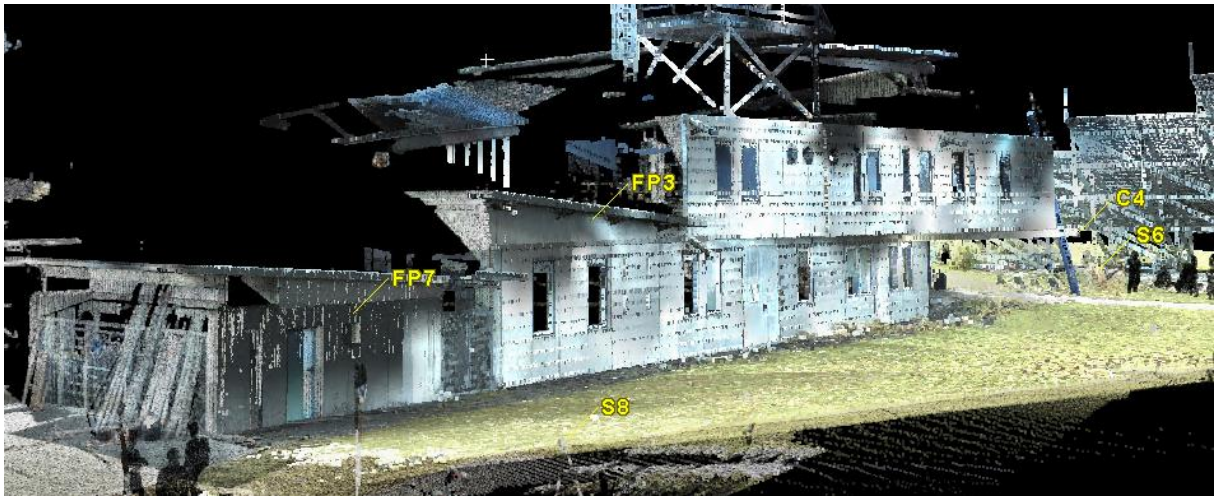

Figure 6 - LiDAR Point Cloud with RGB Information

Problems

The scans were taken by four groups over two days, leading to some inconsistencies between the scans, like marker names or marker heights. Those differences had to be corrected before running a registration of all measurements.

3. Comparison of the Point Clouds

Figure 7 - UAV Point Cloud

Comparing the color information of the two point clouds shown in figure 6 and 7, the colors obtained by the UAV based camera system clearly match the real world more accurately.

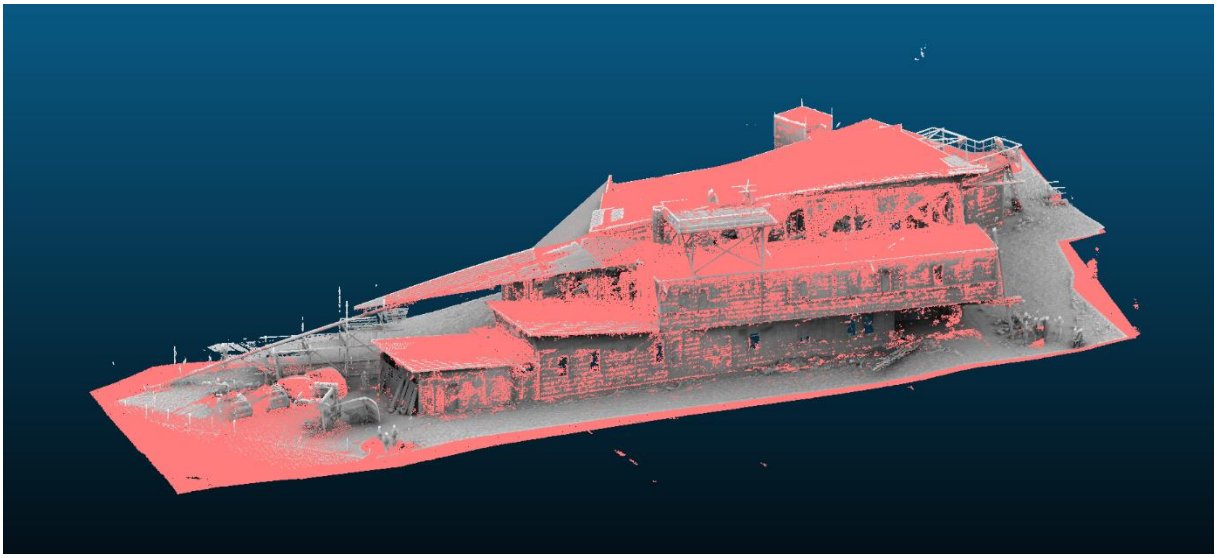

Figure 8 - Comparison of both Point Clouds

When comparing referenced point clouds from both sensors, no significant translations or rotations were found. As expected, there was no LiDAR data (depicted in grey) for the roof of the building, leaving only the red cloud from the photogrammetric method, while the UAV had problems capturing more vertical areas, leading to higher deviations and holes in some parts of the walls, as seen in the top right part of the building in figure 8. Even though we used an oblique camera view, more covered parts like the entrance are still completely missing from the UAV point cloud.

Intensity of the LiDAR point cloud

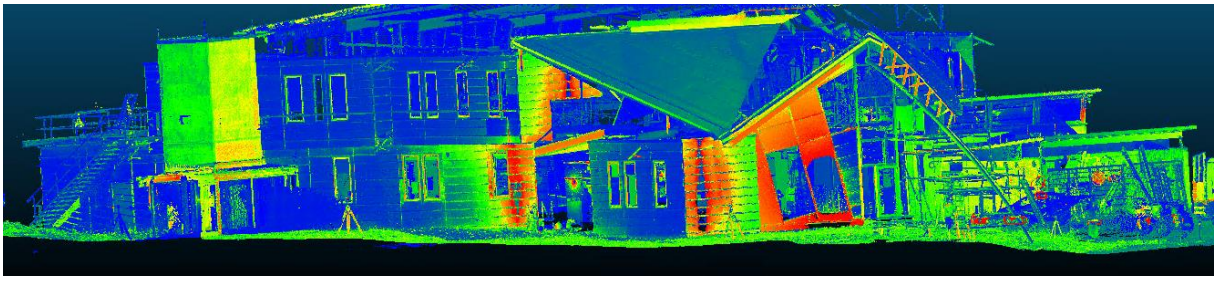

Figure 9 - LiDAR Intensity Point Cloud

As the buildings walls mostly consist of the same metal, the intensity across the model is almost constant, leaving red, high intensity areas only on the parts of the wall directly in front of scanner positions. Consequently, the intensity is pending on distance and angle of incidence on the surface. A high intensity is achieved when the laser hits the surface at a right angle with short distance.

Figure 9 also shows that the metal walls cause far lower intensities than the cement tower on the left. This means the intensity is also based on material properties.

4. Statistical Comparison

Local Noise

To compare the local noise, in each case an assumed plane surface was cut out. For this area a plane was fitted, and an estimate for the variance of the distances of the points to the surface calculated. Roads were best qualified for this.

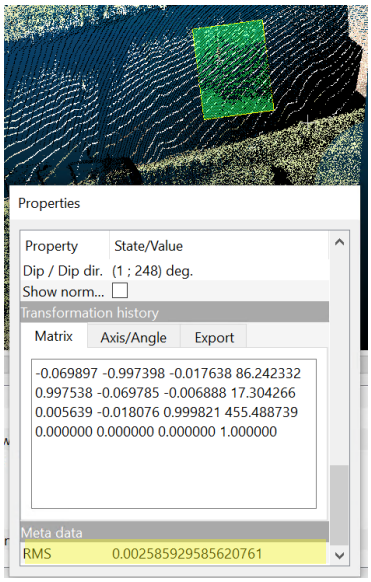

Figure 10 - Local Noise of the LIDAR (Street)

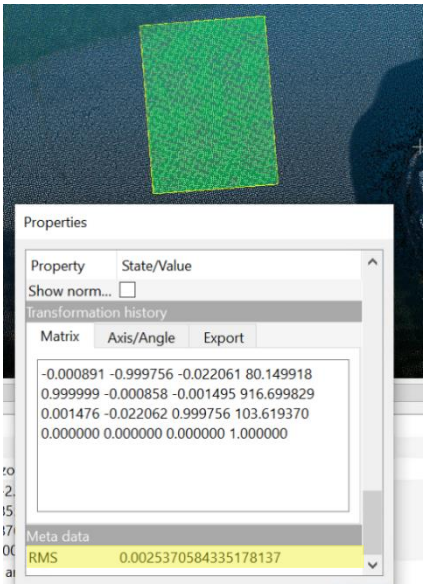

Figure 11 - Local Noise of the UAV (Street)

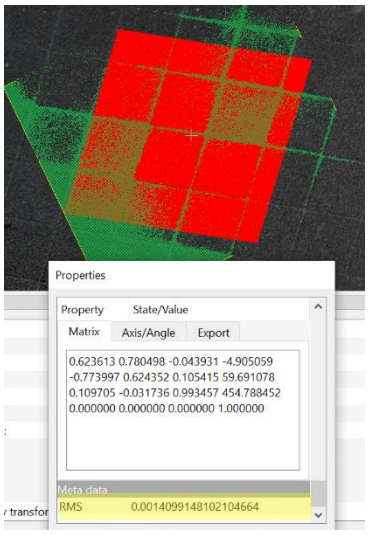

Figure 12 - Local Noise of the LIDAR (Parking Lot)

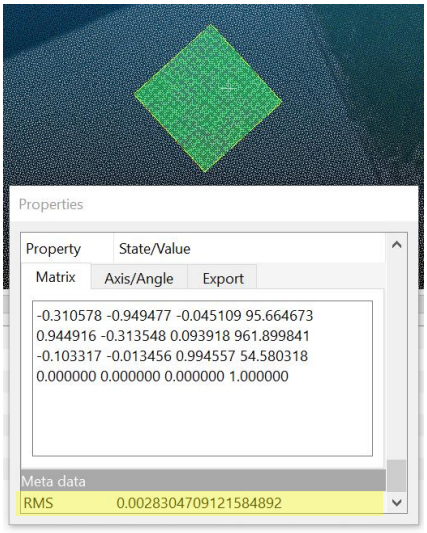

Figure 13 - Local Noise of the UAV (Parking Lot)

For both examples (street and parking area) the calculated standard deviation is lower for the LiDAR cloud then the UAV cloud.

The local noise of the photogrammetric data depends on the image orientation of the dense cloud and on the quality of its image correlation. Because of the large amount of individual measurements deviations can quickly occur. The LiDAR data is only affected by atmospheric influences, which are minimal at short distances.

Point Densities

To compare the point densities of both clouds, a patch of about 1 m² was selected that is well represented in both clouds.

We computed the point densities for a part of the wall on the back side of the building.

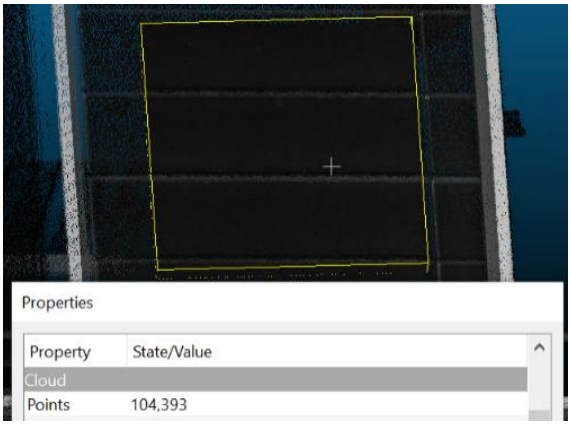

Figure 12 - Point Density of the LiDAR Cloud

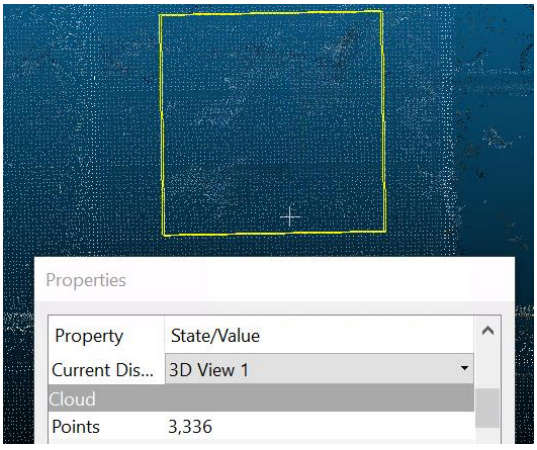

Figure 13 - Point Density of the UAV Cloud

The point density of the scans from the LiDAR sensor is much higher than from the photogrammetric point cloud.

5. Modelling

Finally, a physical 2.5 D model was printed using the 3D printer at the Institute for Photogrammetry.

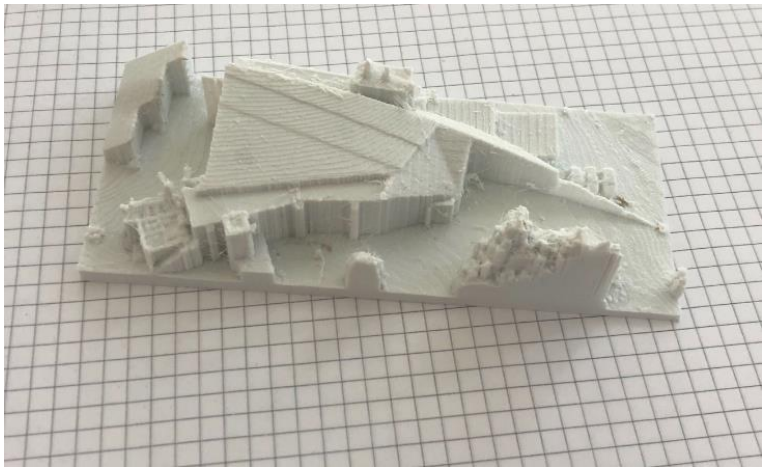

Figure 14 - Printed 2.5 D Modell

Integrated Fieldwork 2020

WP6: GNSS satellite availability

Supervisor:

T.Lambertus

Student:

R.Germann

Contents

1. Introduction

In WP6 the goal was to examine the availability of GNSS satellites near the Hysolar building at the Campus Vaihingen. The groups had to cover different areas using mobile GNSS equipment (rover). Later, the obtained data could be compared to the data of a reference station placed in advance.

2. Fieldwork

The measurements were taken in the area below:

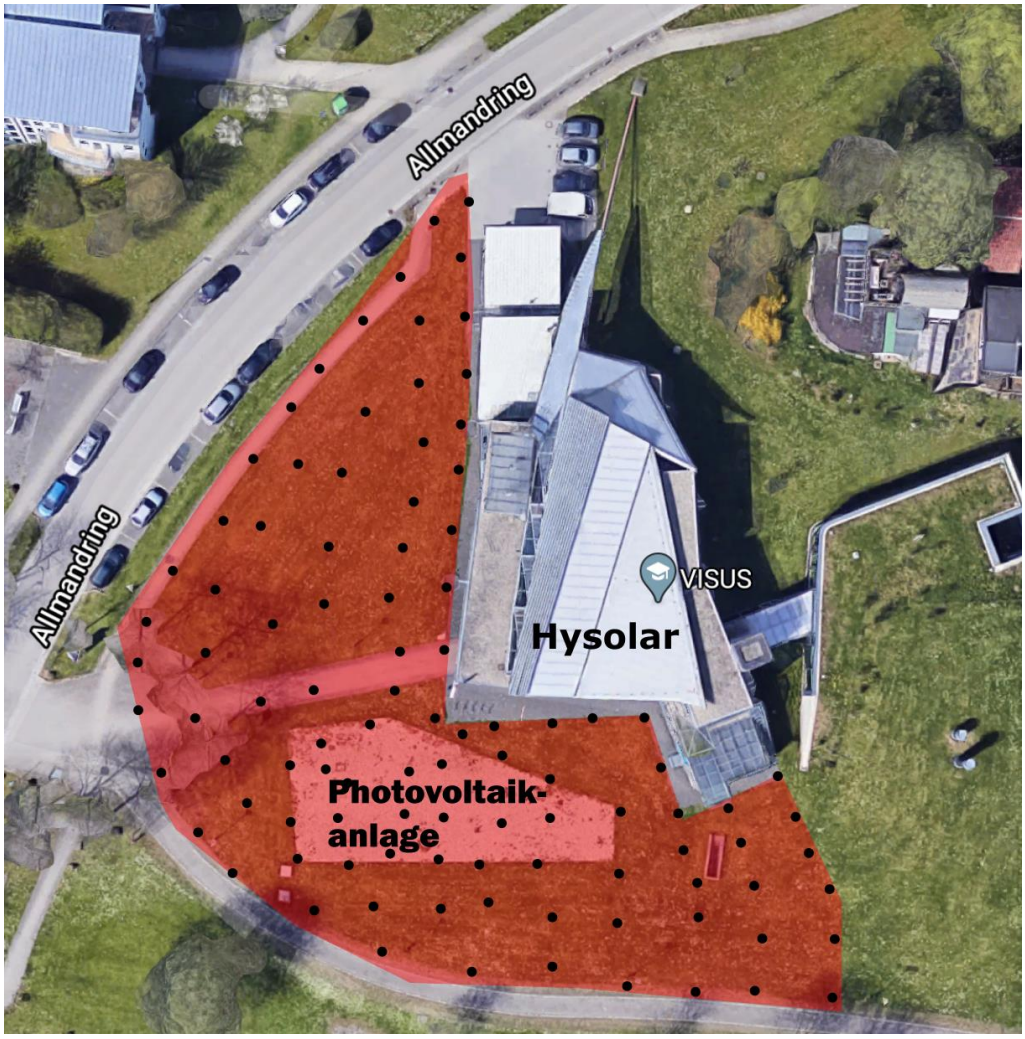

Figure 1: Area for investigation (red), the black points indicate where to measure

Before starting the measurement, it was necessary to set up a base station. This had to be done on a reference point near the green oval with no environmental obstacles, like trees or buildings (see picture below).

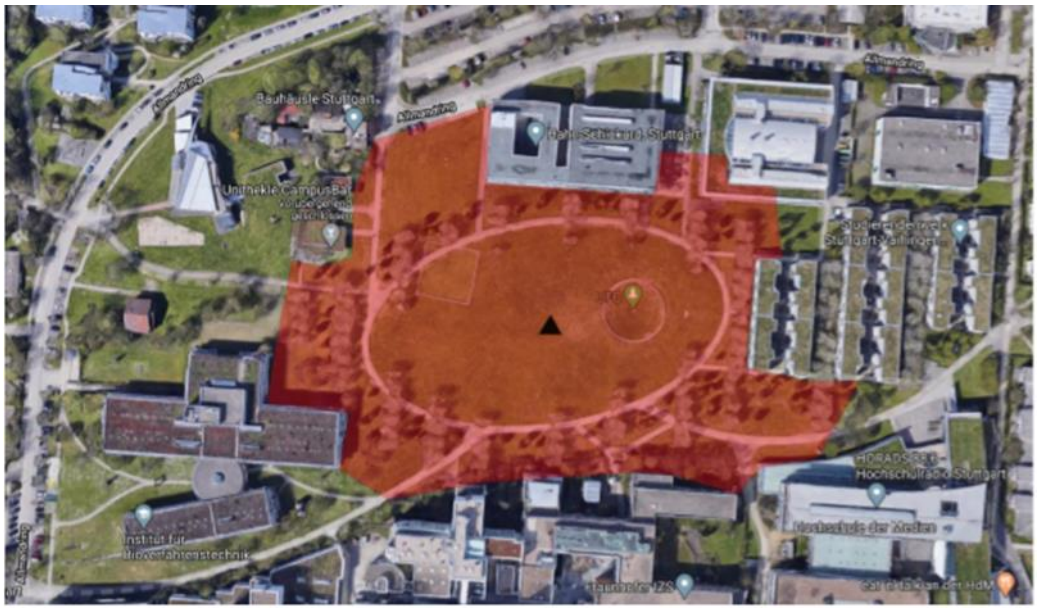

Figure 2: The green oval

The base station was set up with the help of a tripod and levelled. The rover was placed on an antenna rod. Now the notebook and the antenna were turned on. With an active internet connection, it was than possible to access the base and the rover via IP addresses. After that, a software surface was opened, where several settings were done, like RTK settings or corrections (see brief description for details).

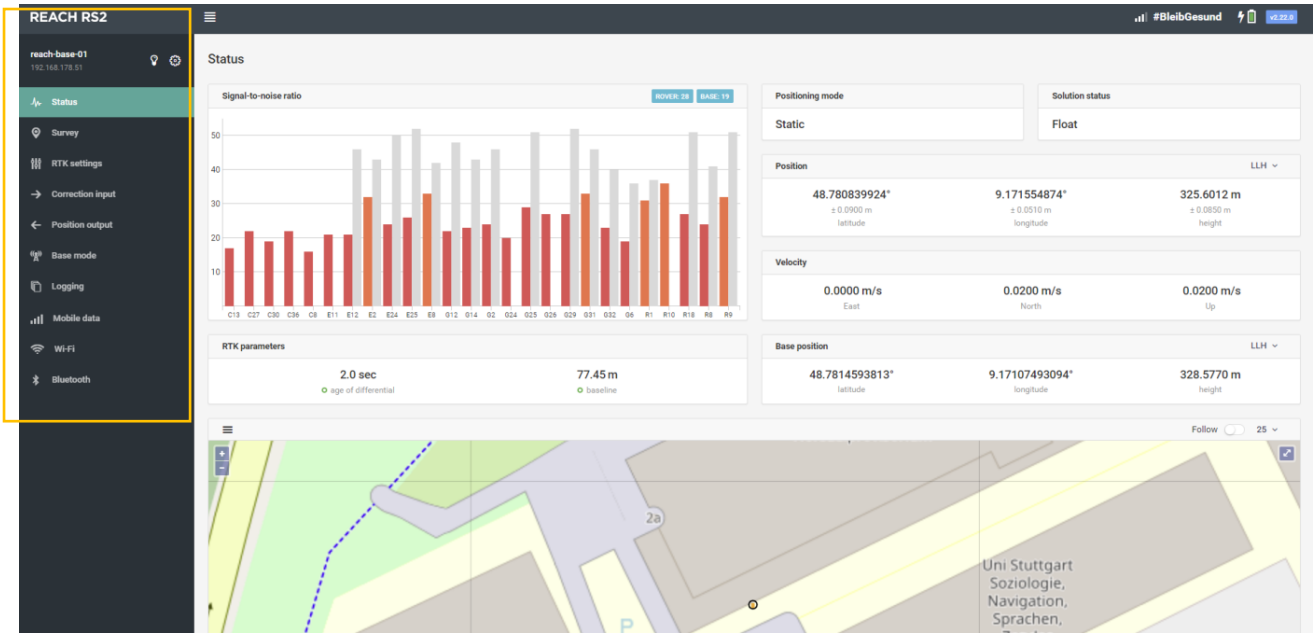

Figure 3: Software surface

The measurement was started through Logging. First, the base position had to be determined. For around 30 minutes, only the base measured. The actual position would be determined later.

During the measurement, one had to make sure that base and rover are connected to each other. Then, points near the Hysolar building were measured with the rover, each one for around 5 seconds and in a 5m grid.

The data was stored automatically in the respective tab on the surface. After finishing the measurement, it was stopped in the Logging data tab.

As a result, each group got LLH data and RINEX data, with nav-Data and obs-data. In the following, only three of the four records could be analyzed, as the base data from one group was missing.

3. Data processing

First, the base position from each group was determined. Therefore, the mean values of Longitude, Latitude and Height from the respective LLH files were calculated. This information is needed afterwards.

For the following steps, the RTK-post and RTK-plot from RTK-lib were used.

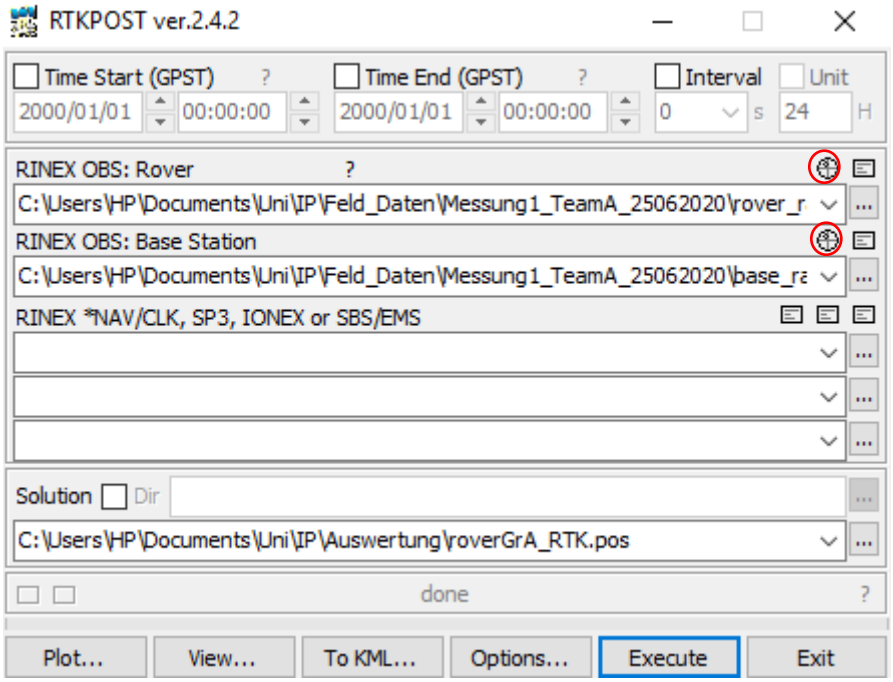

Figure 4: RTKpost

The observation data from Rover and Base were read into the matching tab. In options, for example the base position was set for each group. Also, the data path for the solution had to be set. After the file execution, you can view the calculated coordinates, plot them or convert them in a KML file to show the coordinates in Google Earth.

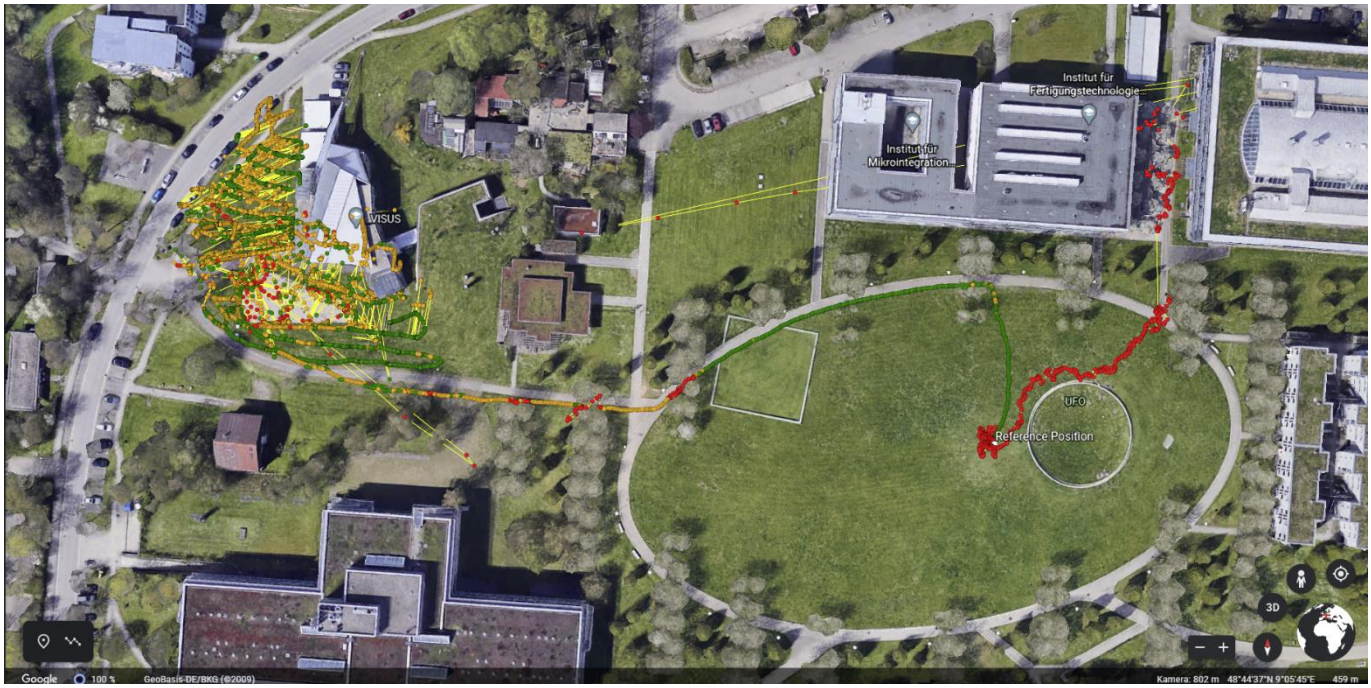

After, the number of available satellites was plotted. Therefore, it was necessary to click the marked symbol above the OBS tabs from rover and base. After enabling several other satellites and changing the first option from SatVis to DOP/NS one could see how the availability of satellites varies over the measurement time. In the following, this is shown for the Rover from Group A.

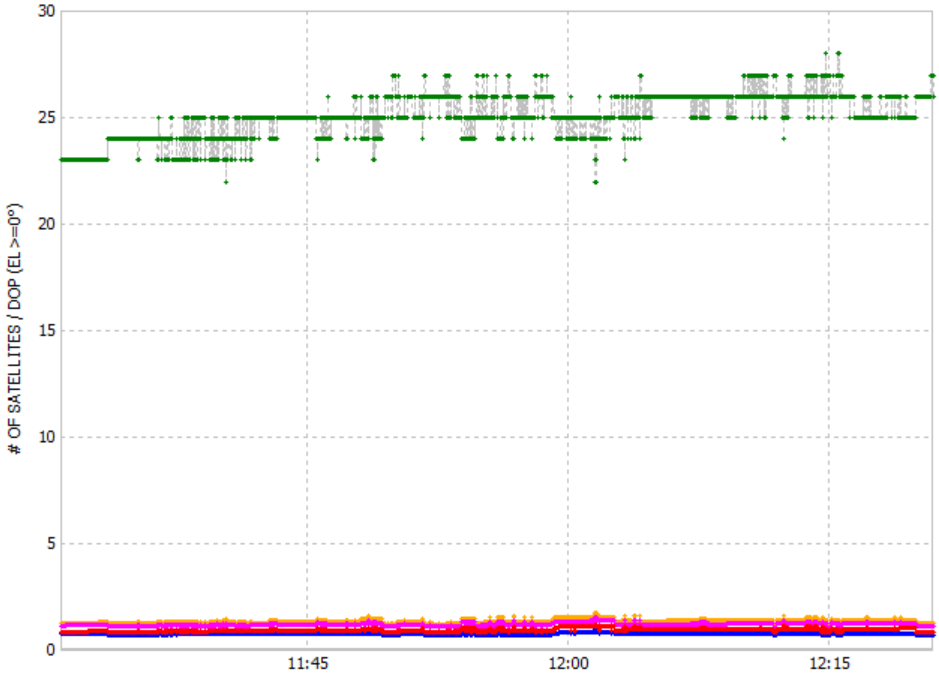

Figure 5: Satellite availability: Rover Group

4. Results

In the following, the results of the different groups will be shown and interpreted.

- Results Group A:

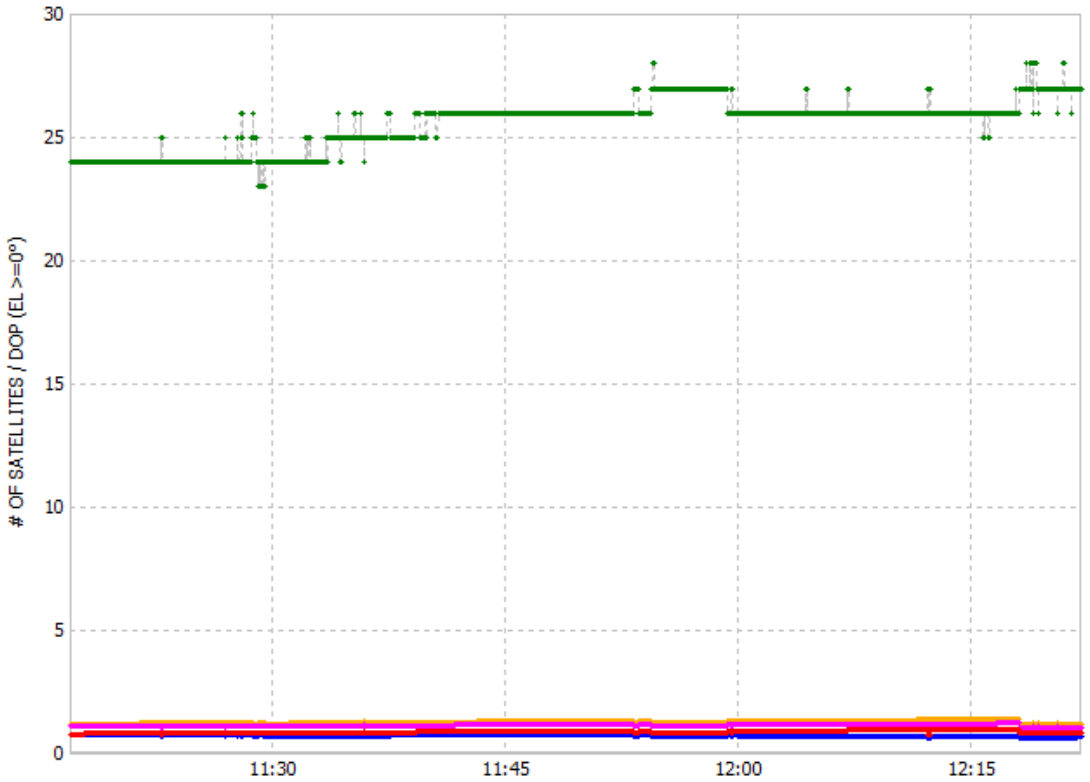

(Base)

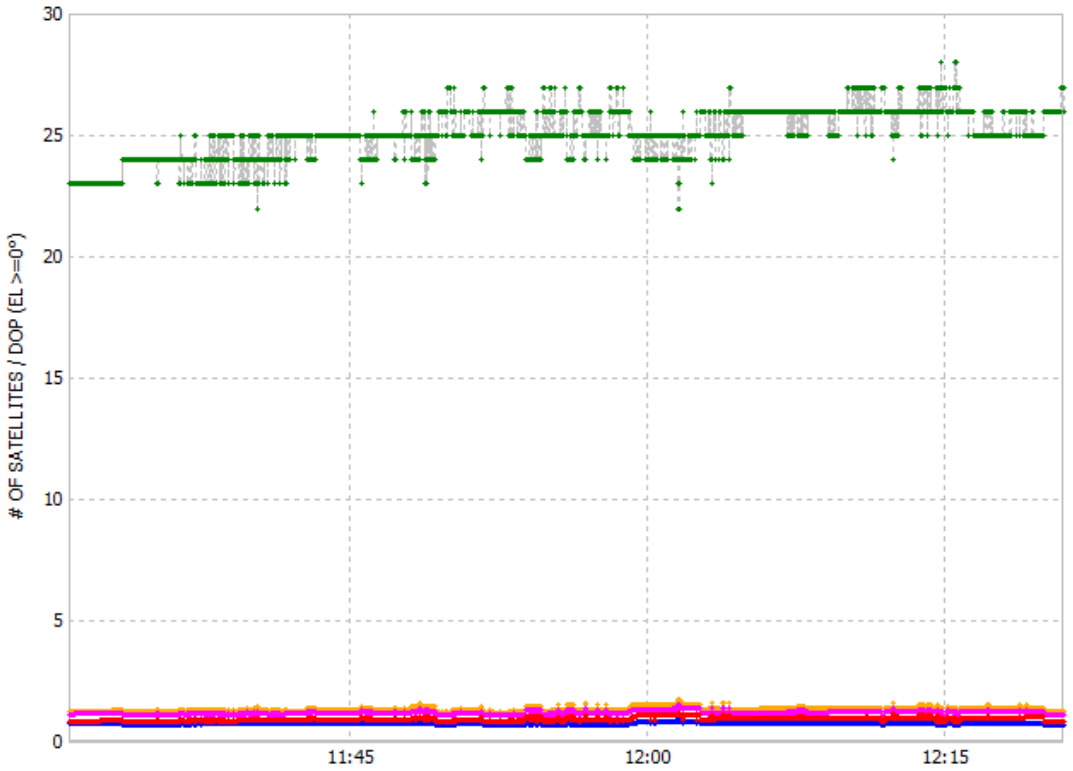

(Rover)

- Results Group C:

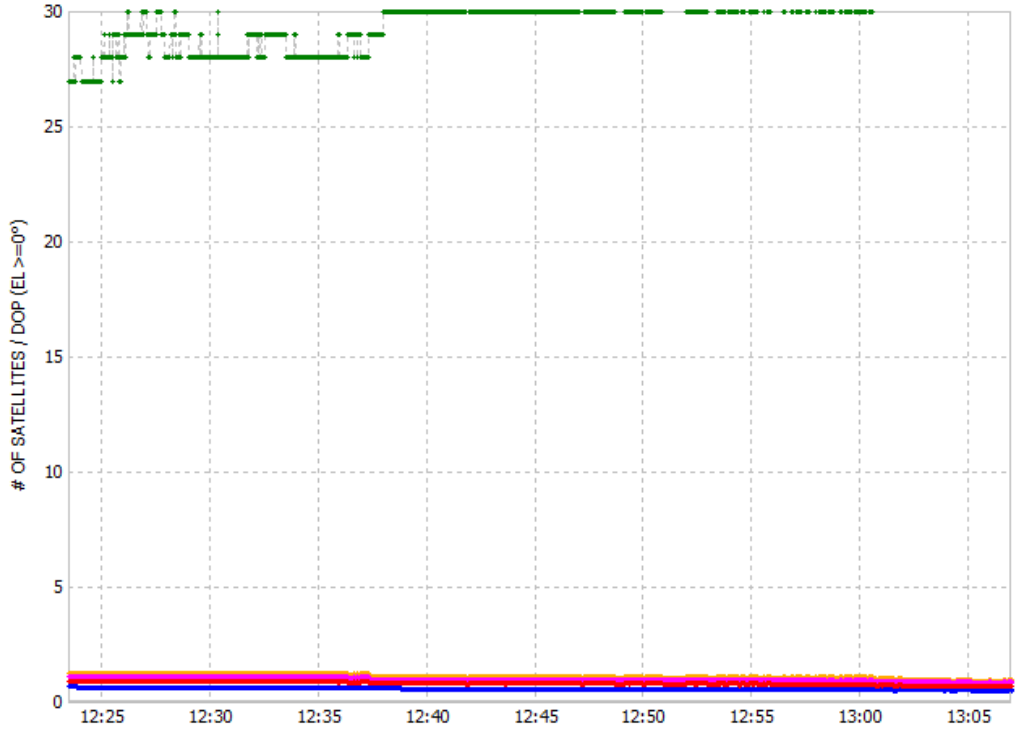

(Base)

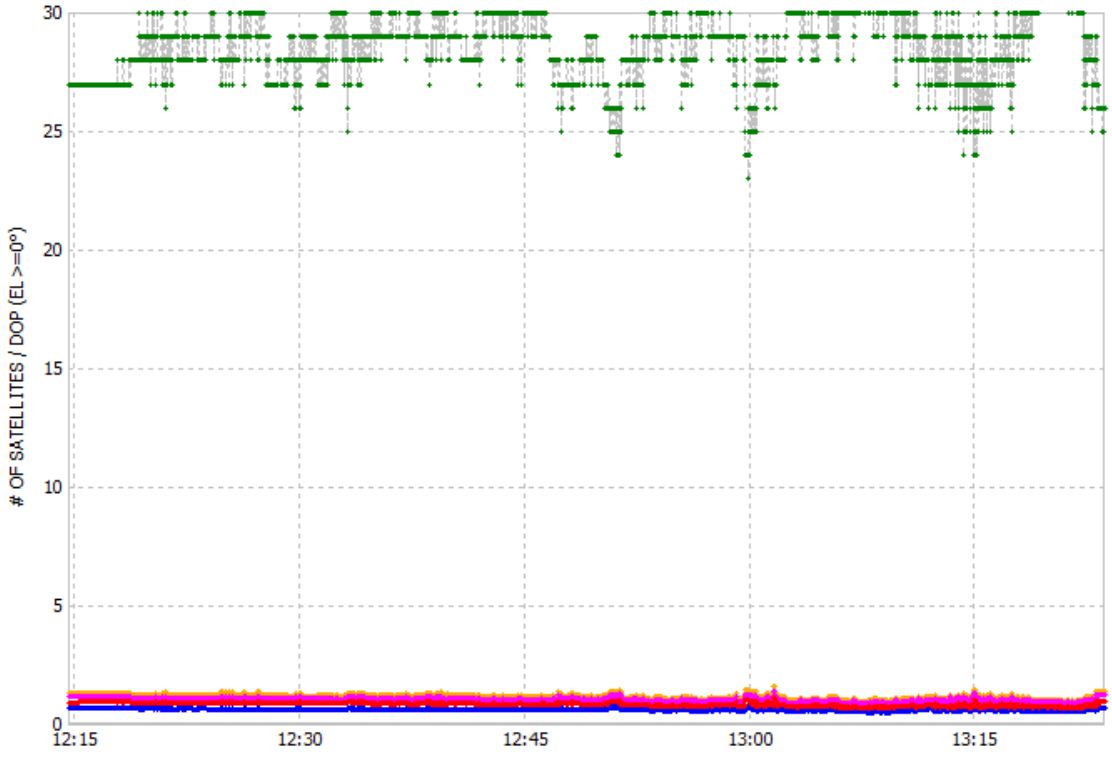

(Rover)

- Results Group D:

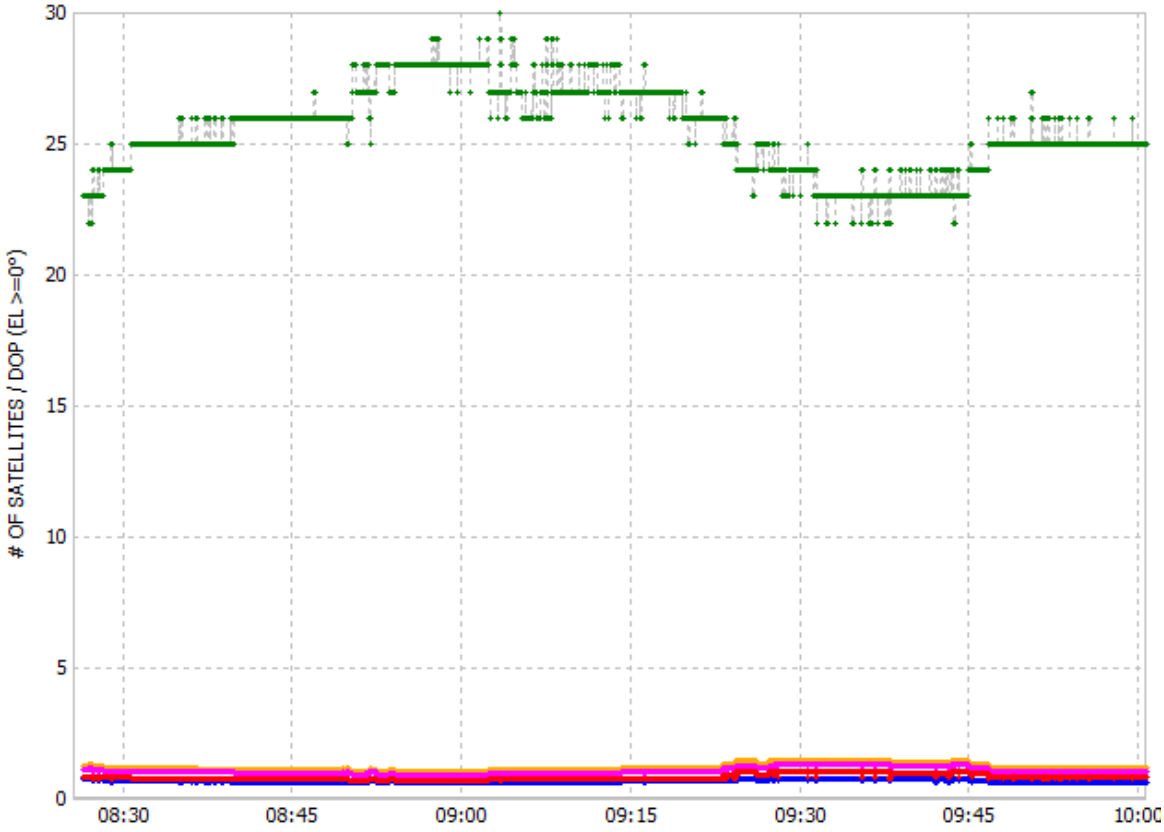

(Base)

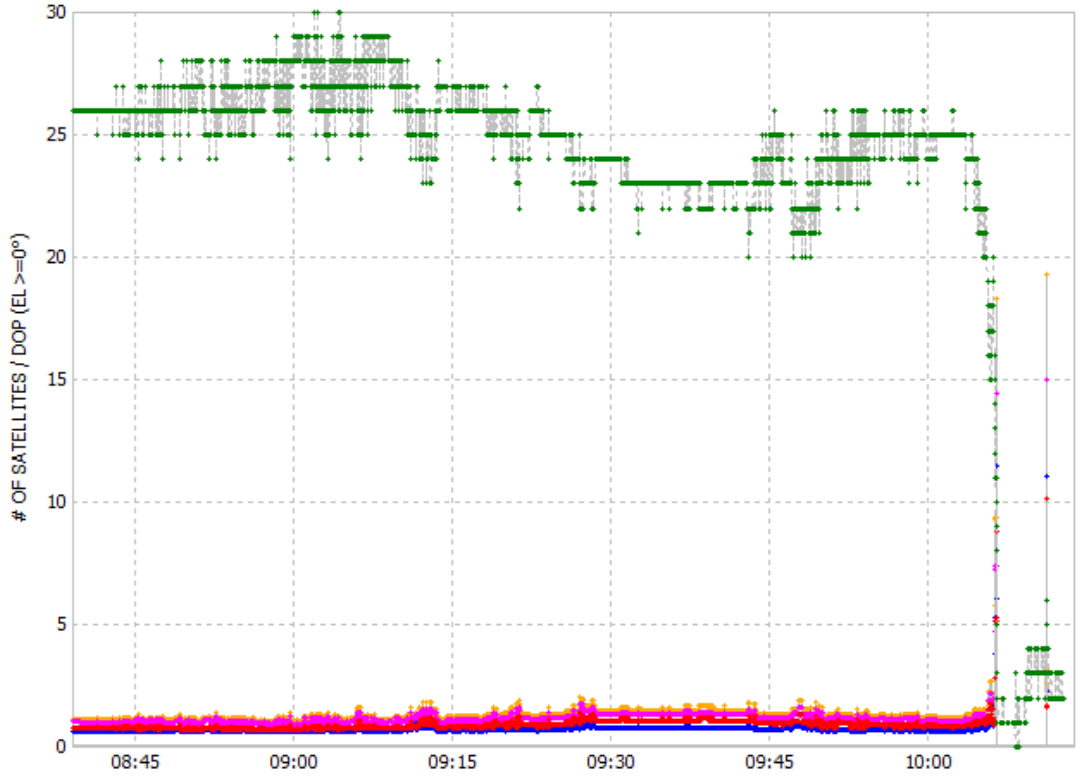

(Rover)

Conclusion:

In summary, one can say that the number of available satellites varied by time in every measurement. Also, the number of satellites measurement taken from the bases does not vary as much as those from the rovers. The reason could be that the base was not moved during, while rover was moved. This could result in errors. In the graphics, it is visible that every group got much more available satellites than the minimum of four, except group D for a small amount of time. One can also recognize low points and high points, which display a very high/low number of satellites. A low number means less available satellites, as for example the receiver is covered by trees or buildings or the satellites signals are reflected by the walls of the Hysolar building. Additionally, a low number of satellites results in big DOP values and vice versa.

Consequently, one can say that is recommended to measure GNSS positions outside, as far as possible from disturbing environmental influences like trees or buildings to obtain a position, which is as accurately as possible.